I&EC research
Industrial & Engineering Chemistry Research

pubs.acs.org/IECR

Review

Recent Impacts of Heterogeneous Catalysis in Biorefineries

Richard Ahorsu, Magda Constanti, and Francesc Medina*

Cite This: *Ind. Eng. Chem. Res.* 2021, 60, 18612−18626

Read Online

ACCESS | Metrics & More | Article Recommendations

ABSTRACT: Renewable biofuel will play a critical role in our energy future by lowering our dependency on fossil fuel because energy shortage is not a remote possibility but is on the horizon. Biofuels are a valuable substitute due to the enormous transportation infrastructure currently in place to support their use and distribution. Apparently, efficient production processes are being developed for both drop-in fuels and fuel additives. Hydrodeoxygenation (HDO) over heterogeneous catalysts provides paths to platform compounds into a range of building block chemicals; however, the selectivity of these reactions is limited due to identical functional groups in intermediate compounds. HDO reactions are complex, as they occur at multiple sites of solid catalysts. Catalyst stability and selectivity toward desirable products are crucial in the design of HDO catalysts. In addition, reduced surface area and phase transformation of catalyst supports could occur with the HDO process. In this review, the exact basis of heterogeneous catalysis is introduced. After that, an insight into how the catalyst's size, porosity, facets, edges, and corners affect selectivity and yields during HDO is provided. Recent strategies in developing heterogeneous catalytic systems to overcome harsh reactions conditions associated with HDO are discussed.

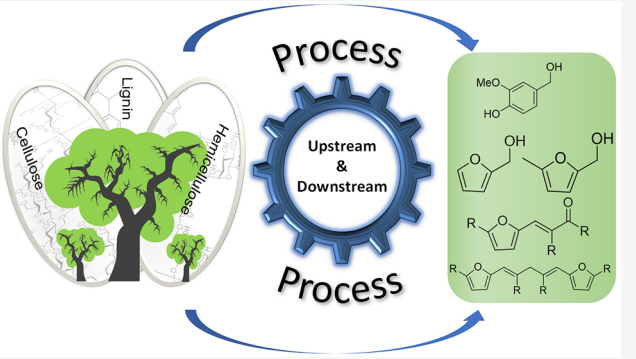

Downloaded via 193.147.222.243 on March 14, 2022 at 15:24:00 (UTC).
See https://pubs.acs.org/sharingguidelines for options on how to legitimately share published articles.

1. INTRODUCTION

Biofuels, derived from lignocellulosic biomass have enormous potential to alleviate the problems associated with our heavy reliance on fossil fuels.[1] Lignocellulose biomass is affordable and abundant and consists of three biopolymers: namely, cellulose, hemicellulose, and lignin.[2] Biomass is a sustainable carbon source used to produce renewable fuels and chemicals.[3] Despite the attractiveness of lignocellulosic substrate as an entry point feedstock in biorefineries, its conversion to liquid transportation fuels is yet to be economically feasible. The current impediment to biofuels development is the lack of cost-effective conversion technologies. Heterogeneous catalysis holds tremendous promise for advancing the commercialization of lignocellulosic biofuels. As a robust bioeconomy develops and next-generation biorefineries are established, heterogeneous catalysis will play a critical role that is analogous to that in petroleum refineries. Catalysis is central to the design of biorefineries, and many new catalysts and catalytic processes are currently being developed. They are founded on knowledge gained over the past decades regarding the efficient upgrading of fossil fuels. This knowledge acquired is used for the availability of new substrates testing and application of novel conversion technologies derived from recent advances and novel concepts developed in the field of heterogeneous catalysis. This review focuses on the application of heterogeneous catalysts on biofuel and biochemical production. The recent advances in catalysis synthesis and applications in the evolution of heterogeneous catalysts from the sub-nanoregime to the nanospectrum, and how to overcome the challenges associated with bioderived fuel process upgrading, are briefly addressed. Many technologies developed in the petrochemical industry require the use of heterogeneous catalysts as a critical step, and this is envisioned to continue in many biorefinery operations. However, due to the unique nature of catalytic processes, their use for biomass and fossil fuel valorization is different and poses some challenges. Two primary approaches to the catalytic valorization of lignocellulosic biomass in biorefinery are as follows: (1) gasification, catalytic combustion, pyrolysis, and liquefaction; these are all thermochemical catalytic treatments that are executed under harsh reaction conditions; (2) low-temperature fractionation of biomass to yield monomer constituents and platform chemicals that are converted into biofuels catalytically.[4] Generally, biomass feedstocks contain a high proportion of oxygenated groups, whereas petroleum feedstocks do not. Liquid fuels from fossil fuels are produced by fractional distillation followed by upgrading through either cracking, isomerization, or alkylation in the presence of heterogeneous catalysts.[5,6] However,

Special Issue: José Luis García Fierro Festschrift

Received: July 16, 2021
Revised: November 14, 2021
Accepted: November 15, 2021
Published: November 29, 2021

ACS Publications

© 2021 American Chemical Society

producing liquid fuels with high energy density from biomass requires the removal of oxygen through various reactions, such as dehydration, decarbonylation/decarboxylation, hydrogenation, and C−O hydrogenolysis.[7] The conversion of monomers and platform chemicals into the target products ordinarily requires a heterogeneous catalytic process.[8] These platform chemicals have varied chemical representations, and their conversion requires specific reaction conditions.

In-depth investigations into the structure−function relationships of heterogeneous catalysts increasingly suggests that catalysts are not only of static surface and bulk structures. On the contrary, they are dynamic entities that can alter their structure in response to the local reaction conditions within the reactor.[9−12] To ensure catalyst stability under the reaction conditions, novel catalyst synthesis concepts must be directed at the atomic, nanoparticle, and catalyst particle length scales. To this end, subnanoparticles (NP) and nanoparticles and their impact, efficiency, selectivity, and challenges are carefully examined to obtain green and sustainable energy from renewable resources such as biomass.

2. HETEROGENEOUS CATALYSTS IN THE NANOSCALE REGIME

2.1. Brief Basics, Principles, and Functions of Heterogeneous Catalysts. Catalysts accelerate the rate of chemical reactions, but they remain unconsumed.[13,14] This definition is still valid. However, as the understanding of the catalyst's size and its impact on reactants and products becomes clearer, the question of whether the catalyst remains the same during and after reaction demands further inquiry. This review does not attempt to address the implication of static and dynamic centers of catalysts; however, it gives a concise account of the current development of heterogeneous catalysts' impact on biorefineries.

Catalytic systems have conventionally been classified as heterogeneous, homogeneous, or enzymatic. Catalysts can be in gas, liquid, or solid form. The catalyst dispersed molecularly in the same phase with the reactants (typically gaseous or liquid) is called a homogeneous catalyst. When the reactants and catalyst are in distinct phases, separated by a phase boundary, it is called a heterogeneous catalysis. The reactants are typically gases or liquids, and the heterogeneous catalysts are solids. The inherent advantage of heterogeneous catalysts is that they exist in a solid state, and thus they are easily separated and recycled from reactants and products.[15,16] However, selectivity and activity are some of the issues associated with heterogeneous catalysts. Heterogeneous catalysts have active sites on the solid's surface, and a high active site concentration per volume is very desirable. The catalytic surface contains various sites, including terraces, edges, vacancies, and kinks, all of which exhibit a range of reactivity and selectivity.[17] Typically, these solid catalysts contain atomic or electronic defects, and atomic representation on their surface and constituents could change during the catalytic reaction. Catalyst's inherent properties include physical, chemical, or dynamic.[18] The dynamic properties are related to the reaction's behavior, including activity and selectivity.[17] Acidity, surface constituents, and the chemical state of the active catalytic phase are chemical properties, whereas density, pore structure, and mechanical characteristics are physical ones.[19] A conventional heterogeneous catalyst consists of three constituents: (1) support, (2) an active phase, and (3) the promoter that increases the activity/stability of the active phase.[20,21] Typically, active phases, containing metal oxides, metals, and metal sulfides with diameters ranging from 1 to 50 nm are dispersed within the pores of supports. These metals, as well as their oxides, carbides, nitrides, and sulfides can specifically catalyze chemical reactions. They have many low-energy surface electronic states[19] that can donate or accept electrons when bonds are formed or broken on the surface.[22] The turnover frequency (TOF), which is typically used to assess catalytic activity, is defined as the number of molecules that react per active site per unit time.[23] TOF is a reaction rate and is proportional to the number of active sites. Even though TOF is a simple tool to compare varied catalysts it often presents some barriers to attempts to compare different catalyst activity data in the literature.[24] The effect of the nanostructure on supported metal catalysts depends on the application: hence, it is categorization into structure-sensitive/demanding reactions and structure-insensitive/straightforward reactions could be necessary.[25] Structure-sensitive reactions are reactions, the rates of which vary according to the size of the particles or the morphology of the active site. On the contrary, the activity of a structure-insensitive reaction does not depend on the catalyst's particle size.[26]

Three factors, namely, activity, selectivity, and stability, usually contribute to the success of a catalyst.[23] The term "activity" is related to the rate of a chemical reaction.[27] The selectivity of a reaction is defined as the proportion of the spent reactant converted to the desired product. Stability is determined by the rate at which the catalytic activity degrades and, thus, the frequency with which the catalyst must be replaced.[28] The atomic composition of a metal catalyst's surface determines its selectivity and activity.[29] Catalyst structures can be settled to promote efficient adsorption and/or beneficial coordination of adsorbates.[30] These processes are substantially controlled by the organization and coordination of surface atoms, and also by the surface density of states related to the various facets. Pt, for instance, has two types of flat surfaces: the Pt [111] facet (hexagonal surface) with six nearest neighbors per surface atom, and the Pt [100] facet (square surface) with four nearest neighbors per surface atom.[22,30] Other authors demonstrated that while the hexagonal surface was seven times more active than the square surface in the aromatization of *n*-pentane to toluene, the square surface was four to seven times more active in the isobutane to *n*-butane isomerization reaction.[22] Careful tuning of surface facets could synergistically improve catalytic performance in regarding selectivity and reactivity. In addition, the porosity, or shape of the catalyst's pores, can affect the catalyst's catalytic properties. Here, the support on which the active phase has been immobilized determines the porosity and shape of pores. Support "effect" is defined as an interaction between the support or carrier and the active catalytic phase leading to a change in TOF.[25] Boudart[25] categorized metal−support interactions into six distinct types: (1) strong interaction of an unreduced metal oxide with oxide, (2) support-induced size and morphology, (3) contamination of the metal by the support material during the catalyst's preparation or reduction, (4) catalysis with bifunctionality, (5) species spillover from metal to support and vice versa, (6) a change in the electronic properties of small crystallites caused by close contact with the support.[31]

An ideal catalyst should operate cyclically in the process. Heterogeneous catalyst activity or selectivity deactivates over time, a process known as deactivation. There are five causes of deactivation: poisoning (potentially reversible), fouling (often reversible), active site reorganization (potentially reversible),

https://doi.org/10.1021/acs.iecr.1c02789
Ind. Eng. Chem. Res. 2021, 60, 18612−18626

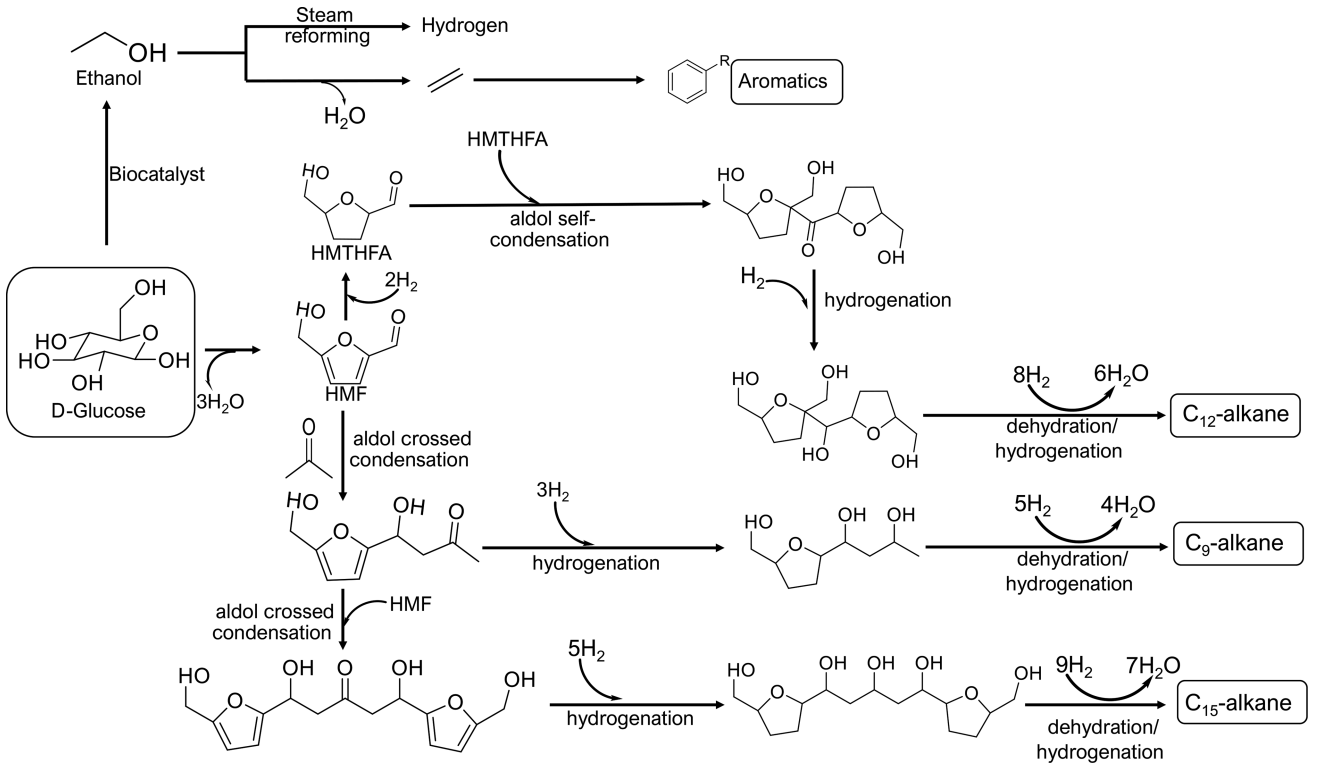

Figure 1. Schematic pathway for valorizing platform chemicals to liquid fuel and aromatics. 5-hydroxymethylfurfural (HMF), 5-hydroxymethyltetrahydrofurfural (HMTHFA). Figure adapted with permission from ref 38. Copyright 2005 The American Association for the Advancement of Science.

hydro(thermal) dissolution (irreversible), and active phase leaching (irreversible).[28,32,33] Deactivated catalysts can be regenerated.

3. ROLE OF NANOCATALYSTS IN BIOMASS CONVERSION INTO BIOFUELS

While catalysis has made significant contributions to the petrochemical industry, it is still in its infancy in biorefinery applications. Thermal catalysis is very important for the biomass-to-fuel conversion process. Biomass feedstocks are processed under reaction conditions more varied than those for petroleum feedstocks, temperature and pressure being the most crucial parameters. Among the many thermochemical processes, pyrolysis is commonly employed in the conversion process[34,35] because it is an efficient method of converting substantial amounts of wood into bio-oil, that can further be catalytically transformed into biofuels and chemicals. However, bio-oil has many disadvantages, such as having increased levels of oxygen and water, corrosive properties, decreased stability, high viscosity, low calorific value, and incompatibility with crude oil-based fuels.[36] Thus, the quality of bio-oil needs to be improved before it can be upgraded to biofuel. There are four methods for enhancing bio-oil: (i) fluidized catalytic cracking (FCC), (ii) decarboxylation (DCO), (iii) hydrodeoxygenation (HDO), and (iv) hydrotreating (HT).[37] Because hydrogen in refineries may come from crude oil, HDO processing of bio-oil may be impractical in maintaining a green and sustainable process. DCO of bio-oil to high-quality hydrocarbons, using ZSM-5 and USY zeolites catalysts is a promising method for producing an enhanced bio-oil that is more stable, less corrosive, and with high energy. Nevertheless, this process produces a substantial amount of coke.[37] Thus, new catalysts for exhaustive decarboxylation of bio-oil are needed to make the catalytic system economically feasible. Conventionally, thermal conversion processes are employed to produce bio-oils. Solid catalysts have increased catalytic activity and can easily be separated from the products. Acid-functionalized paramagnetic nanoparticles are reassuring candidates for use in biomass catalytic hydroconversion. Monodispersed nanocatalysts have excellent access to the oxygen atoms in the cellulose−ether linkage, owing to their fluidity. Noble metal-doped catalysts could assist bio-oil reactions that involve removal of oxygen, ring-opening, and minimize hydrogen consumption.[37] However, biomass feedstock has lower thermal stability as compared to petroleum feedstock; thus, making it difficult to process them in the gas phase. Liquid phase valorization of biomass feedstock into fuels and chemicals is desirable.

The subsections that follow cover recent advances in valorizing biomass into platform chemicals and subsequent upgrading into fuels and valuable commodities with nanoparticles (see Figure 1).

3.1. Nanocatalyst-Assisted Biomass Valorization.

3.1.1. Metal Nanoparticles Application. A metal-based nanocatalyst's activity predominantly depends on its size, shape,[11] morphology, composition,[39] and surface modification. Besides from the size and shape of nanoparticles, key parameters affecting the catalytic performance of nanocatalysts include both acidic and alkaline properties, the category and content of metal(s), and porosity. The metals' ability to exist in various stable oxidation states is the main reason for their widespread use in catalytic processes, specifically in oxidation and hydrogenation. In HDO, the C−C bond is cleaved via decarbonylation, and various functionalities are hydrogenated (−COOH and RCOR[1]).[40−42]

https://doi.org/10.1021/acs.iecr.1c02789
Ind. Eng. Chem. Res. 2021, 60, 18612−18626

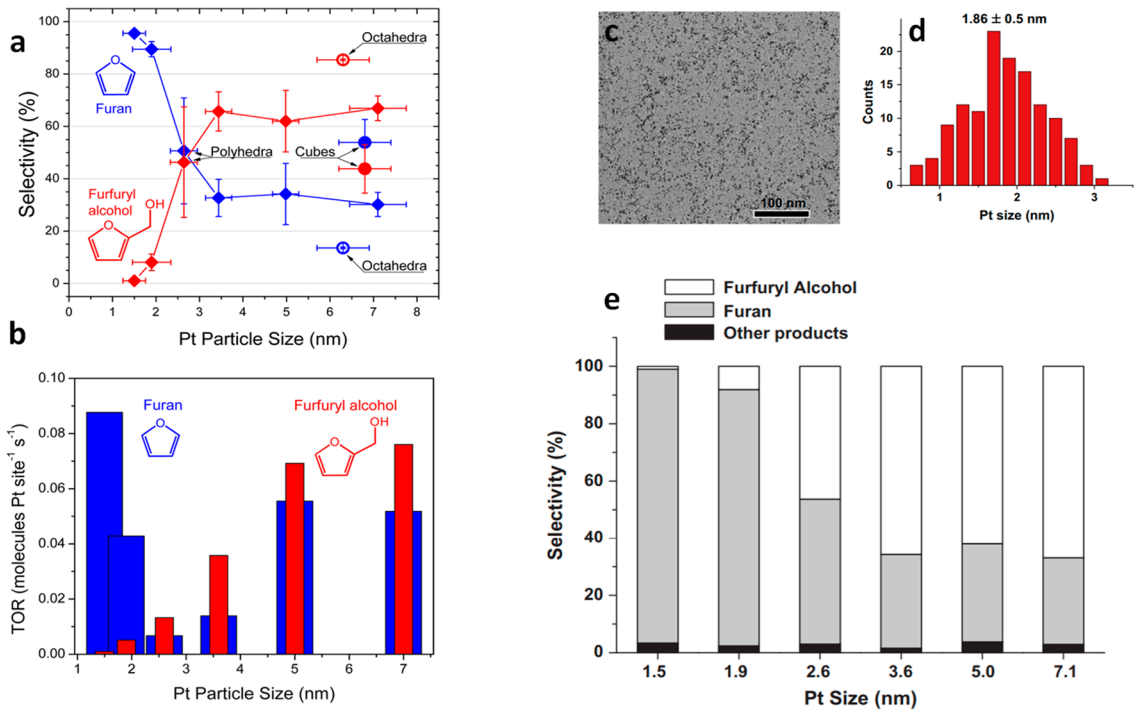

Figure 2. Plot of selectivity to furan and FOL against projected Pt particle size (nm) (a); plot of TOR values versus mean Pt particle size (nm) (b); TEM image of PVP-capped Pt-NP (c); histogram distribution of PVP-capped Pt-NPs (d); plot of product selectivity of furfural hydrogenation reactions over Pt-NP on mesoporous oxides as a function of size (e). Panels a and b adapted from ref 47. Copyright 2012 The American Chemical Society. Panels c–e adapted with permission from ref 48. Copyright 2013 Elsevier.

Table 1. Assessment of Catalyst Performance for Hydrogenation and Hydrodeoxygenation of Furfural (FF) to Furfural Alcohol (FOL), 2-Methylfuran (2MF) over Different Solid Catalysts

catalyst	size[a] nm	reaction type	reaction phase	conversion (FF) (%)	selectivity (%)	ref
CuOAl	7–12	hydrogenation	liquid	>99	>99 FOL	57
ZnOAl	7–10	hydrogenation	liquid	>99	>99 FOL	57
$Zr(OH)_4$ @Co	na	hydrogenation	liquid	93.9	97.3 FOL	58
20%Ni/Bentonite	na	hydrogenation	liquid	99	98 FOL	59
$(350H_2)Ru_3Co_{100}$	ca 3	hydrogenation	liquid	98–100	98–100 FOL	60
Au/Cu–Al_2O_3	ca 3	hydrogenation	liquid	100	100 FOL	61
Pt@g–C_3N_4	4.25	hydrogenation	liquid	100	>99 FOL	62
Cu–Mg–Al	na	hydrogenation	liquid	100	100 FOL	63
Cu_xNi_y/MgAlO	5.2	hydrogenation	liquid	>99	>100 FOL	64
NiCoB alloy	29.7	hydrogenation	liquid	91.3	82.0 FOL	65
Co/SBA-15	na	hydrogenation	liquid	95	96 FOL	66
Ru/UiO66	<3	hydrogenation	liquid	94.9	>99 FOL	67
$RuSn_{0.4}$/C	2.7	hydrogenation	liquid	95	>85 FOL	68
Pd–Cu–MgO	na	hydrogenation	liquid	100	98 FOL	69
Pt/(Fe,Co)–BTC	1.7	hydrogenation	liquid	98	99 FOL	70
NiPMoS	na	HDO	liquid	94	– 2MF	71
$CoMo/Al_2O_3$	na	HDO	vapor	27.8	100 2MF	72
NiZn alloy	7.8	HDO	liquid	95	91 2MF	73
$Ni_2P\_0.5$	na	HDO	liquid	100	83.1 2MF	74
$Cu/CuFe_2O_4$@C-A	6.3	HDO	liquid	100	100 2MF	75
NiMo IMC	18.6	HDO	liquid	100	99	76
Ni_2P-1.00–300	<95	HDO	liquid	100	91.2	77

[a]Note. na = not available/size above 100 nm.

We demonstrate many ways of how rational design of metal nanoparticles can aid to transform lignocellulosic biomass in this review. Glucose and xylose are critical intermediate compounds in the transformation of biomass that can be converted into fuels and other building-block compounds.[43] HMF and furfural, a breakdown product formed when glucose and xylose are dehydrated, have recently garnered considerable attention due to their potential for conversion into liquid hydrocarbons[44] and valuable renewable precursor compounds.[45,46] Investigation on the effect of different Pt NPs on furfural alcohol (FOL) and

https://doi.org/10.1021/acs.iecr.1c02789
Ind. Eng. Chem. Res. 2021, 60, 18612–18626

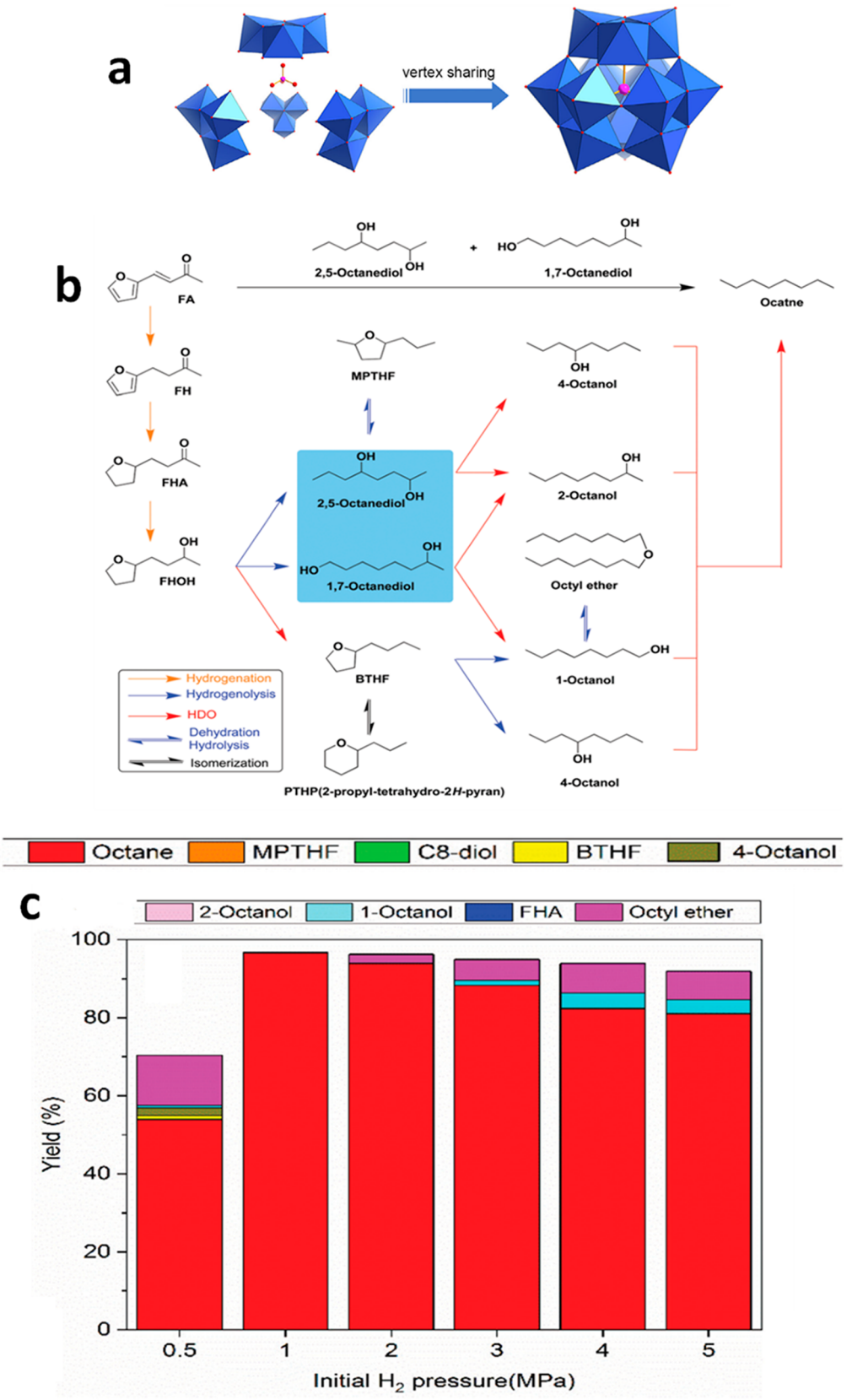

Figure 3. Schematic of a disassembled structure of α-keggin type polyoxometalate (a); octanediol-route for the HDO of 4-(2-furyl)-3-buten-2-one with Pd/C−HPW , Furfural-aceone adduct (FA), 4-(tetrahydrofuryl)butan-2-ol, 4-(tetra-hydrofuran-2-yl)butan-2-one (FHOH), 2-methyl-5-propyl-terahydrofuran (MPTHF) and 2-butyltetrahydrofuran (BTHF) (b); influence of initial H_2 pressure on the HDO of 4-(2-furyl)-3-buten-2-one over Pd/C−HPW. Experimental conditions: 4-(2-furyl)-3-buten-2-one (100 mg), Pd/C (50 mg), HPW (50 mg), cyclohexane (10 mL), 130 °C, 400 rpm, 4

https://doi.org/10.1021/acs.iecr.1c02789
Ind. Eng. Chem. Res. 2021, 60, 18612−18626

Figure 3. continued

h (c). Panel a adapted with permission from ref 81. Copyright 2019 Elsevier. Panels b and c adapted with permission from ref 79. Copyright 2021 The Royal Society of Chemistry.

furan selectivity revealed that Pt particles (<2 nm) formed primarily furan, while polyhedral Pt particles (>3 nm) produced mainly FOL.[47] FOL selectivity was highest for 6.2 nm Pt NPs with octahedral architecture, while 6.8 nm Pt NPs with cube architecture show much less selectivity[47] (see Figure 2a). The selectivity of furfural alcohol increased to 66% at set reaction conditions (200 °C, 0.93 bar H_2, Pt NP diameter 1.5 nm to 7.1 nm), and TOR was 70 times higher (see Figure 2b).[47] Furan was the main product for 1.5 nm Pt NP in another study, while FOL was preferred for bigger particles[48] (see Figure 2c−e). FDCA production from furfural conversion over Pt-PVP NPs catalysts having diameters between 1.5 and 5 nm was reported.[49] Both aldehyde and hydroxyl group oxidation were considerably improved when particles were smaller. Pt-PVP NPs with a diameter of 1.5 nm produced 95% FDCA.[49]

To highlight structure−reactivity relationships, the liquid phase selective hydrogenation of furfural to FOL over silica supported Ru nanoparticles was comprehensively explored recently.[50,51] Even though FOL was selectively produced over Ru NPs of various sizes between 2−25 nm, the conversion of furfural was dependent on the surface fraction of Ru, showing the apparent sensitivity of the catalyst structure.[50,51] FOL and its competitive decarbonylation to furan demonstrate opposing structure sensitivities; that is, carbonyl hydrogenation is favored by larger Ru nanoparticles (>17 nm), whereas furan is favored by smaller Ru nanoparticles (≤17 nm), irrespective of the support textural properties. The decarbonylation activity depends on the particle dimensions. This opposed pattern of product distribution was due to the separate parts of low-coordinated sites on the variedly sized NPs. Scott et al. synthesized two series of Pd/TiO_2 catalysts from two different systems: only water (A-series) and ethanol−water (B-series) system.[52] By modifying the preparation's solvent system (ethanol−water), a greater fraction of corner and edge sites, which can regulate product selectivity in furfural hydrogenation can be achieved.[52] In addition, it was discovered that the selectivity profile was not simply related to particle size; for the B series, FOL selectivity reduces as particle diameter increases, while the A series has the opposite relationship.[52] Thus, the available sites were determined not only by particle size, but also by the interaction of the protecting agent with the prepared NPs.[52] Both the nature of the support (carbon, MgO, TiO_2, and Al_2O_3) and the addition of Pt affected the efficiency of Pd catalysts for liquid-phase hydrogenation of furfural as observed by Albilali et al.[53] The impact of catalyst size on furfural conversion and product selectivity of recent published works has been summarized in Table 1.

3.1.2. Nanoscale Metals/Metal Oxides Catalysts for Furan Upgrading to Biofuels. Converting biomass to high-density fuels typically involves a series of steps, such as alkylations, oligomerizations, condensations, and hydrogenations.[54] Catalysts are critical for efficiency, selectivity, and yield in all these processes.[54−56] Cyclopentanone is another important lignocellulosic compound usually synthesized via aqueous-phase selective hydrogenation of furfural derived from hemicellulose hydrolysis of forest residue and agricultural waste. Cyclopentanone can be used as a starting material in the synthesis of high-range cycloalkanes for jet fuel. Direct production of a polycycloalkane, tri(cyclopentane), using lignocellulose-derived cyclopentanone was accomplished in a continuous flow reactor with two beds.

The first bed was employed to convert cyclopentanone selectively to 2,5-dicyclopentylcyclopentanol using a Pd−MgAl−HT catalyst.[78] A high carbon yield of 81.2% for 2,5-dicyclopentylcyclopentanol was obtained under solvent-free and mild conditions.[78] Furthermore, 2,5-dicyclopentylcyclopentanol was hydrodeoxygenated to give tri(cyclopentane) with a carbon yield of 80.0%.[78] Among the catalysts studied, Ni−Hβ−DP, synthesized via deposition−precipitation (DP) had the highest activity for the hydrodeoxygenation step.[78] This polycycloalkane can be used as a fuel enhancer. Recently, with the use of a single-pot transformation of bioderived furans at low temperatures, a novel octanediol-route was achieved to manufacture octane.[79] By catalytic transformation of furans with Pd/C and phosphotungstic acid (HPW), a 96.6% yield of octane was achieved,[79] (see Figure 3). It was postulated that the presence of water improved the association between acids and metals, and also caused rapid transfer of hydrogen: thus allowing the cleavage of the C−O bond at mild temperatures.[79] Through the terminal W = O structure, close association between HPW and Pd/C was formed without weakening the Keggin structure's integrity: hence, facilitating HDO at mild temperatures.[79] 1-(3-cyclopentyl)cyclopentyl-2-cyclopentylcyclopentane, a high-density fuel, was first synthesized with cyclopentanone giving a carbon yield of 70%.[80] The first step was to synthesize 2-cyclopentyl cyclopentanone using cyclopentanone and hydrogen in a one-pot reaction catalyzed by Raney metal and alkali hydroxides to obtain 2-cyclopentyl cyclopentanone.[80] The second step produced of 2-cyclopentyl-5-(2-cyclopentylcyclopentylidene)-cyclopentanone via self-aldol condensation of 2-cyclopentyl cyclopentanone under vacuum and solvent-free conditions.[80] Under solvent-free conditions, the 2-cyclopentyl-5-(2-cyclopentylcyclopentylidene) cyclopentanone underwent hydrodeoxygenation in the third step over the $Ni-SiO_2$ catalyst to give 88.5% yield of 1-(3-cyclopentyl)cyclopentyl-2-cyclopentylcyclopentane and 99.0% yield of polycycloalkanes.[80]

The $Ni-SiO_2$ catalyst was stable under reaction conditions.[80] Aldol condensation and hydroxyalkylation-alkylation (HAA) are two efficient processes for increasing the carbon chain of furfural prior to its conversion to biofuels.[82] HAA in conjunction with HDO is a clean alternative path to high-quality diesel or jet fuel synthesis.[82] To apply HAA-HDO processes, various resins (Nafion, Amberlyst, and others) were employed to couple 2-MF and furfural.[83] The highest activity and stability were reported for the Nafion-212 resin. Pd/C, Pt/C, and Ni−WxC/C catalysts were used for the HDO of hydroxyalkylation/alkylation products, with the Ni−WxC/C catalyst showing the best catalytic performance and stability.[83] The Dumesic group devised a stepwise aldol condensation and hydrogenation method that used a bifunctional $Pd/MgO-ZrO_2$ catalyst for furfural upgrading in the aqueous medium.[84] After the hydrogenation of products generated from cross aldol condensation of acetone with furfural, a total carbon yield of products greater than 80% was achieved.[82,84] Recently, microwave-assisted aldol condensation of furfural and acetone was reported to give cross products of furfuryldeneacetone and 1,5-

https://doi.org/10.1021/acs.iecr.1c02789
Ind. Eng. Chem. Res. 2021, 60, 18612−18626

bis(2-furanyl)-1,4 pentadien-3-one under mild reaction condition (temperature 100 °C, the ratio of furfural to hydrotalcite catalyst was 2:1). A 100% conversion of furfural was achieved after 30 min of reaction with ca 95% yield of furfuryldeneacetone.[85] Both acid and alkaline solid catalysts with different particle sizes played a role in the product selectivity during the aldol condensation reaction, (see Table 2). 2,5-Dimethylfuran

Table 2. Aldol Condensation of Furfural (FF) with Acetone over Different Solid Catalysts

catalyst	temp (°C) / time (h)	FF con (%)	FAc sel (%)	FA_2C sel (%)	ref
Sn-Beta	160/2	99	40.0	22.0	92
ZnO−Al_2O_3	80/4	3.2	99.9	0.1	93
ZnAlLa-1	80/4	73.0	86.7	13.3	93
ZnAlLa-2	80/4	91.0	61.7	38.3	93
ZnAlLa-2	100/4	93.9	43.1	56.9	93
Mg−Zr	50/24	81.4	14.4	61.5	94
Pd−Mg−Zr	50/24	73.4	29.2	30.6	94
Mg−Al	50/24	63.8	31.1	42.9	94
Pd−Mg−Al	50/24	54.7	11.9	3.0	94
Mg−Al (1:3)[a]	100/2	>95	∼73	∼22	95
Mg−Al (1:3)[b]	100/2	∼35	∼50	∼12	95
MgAl (1:3)[c]	100/2	∼50	∼54	∼14	95
Py−Mg−Fe	50/4	88		34	96
La_1Mg_3MO-H	150/7	96	98		97
3MgAl−HTC	55/3	>95	∼50	∼38	98
Cu−BTC	100/2	2.7	70	0	99
Fe−BTC	100/2	26.2	71	20	99

[a]Calcined catalyst. [b]Rehydrated catalyst (H_2O), [c]Rehydrated catalyst (vapor). Abbreviations: FAc = furfuryldeneacetone, FA_2C = 1,5-bis(2-furanyl)-1,4 pentadien-3-one, sel = selectivity, con = conversion.

(DMF) is a highly attractive furan derivative and is used in gasoline blends. A newly developed bimetallic system using soft templating to encapsulate PtCo NPs in hollow carbon spheres was realized, (see Figure 4). During the carbonization process, Pt NPs were in situ impregnated into the spheres, and subsequently Co NPs were added as-prepared Pt@HPS.[86] Pt@HPS was transformed into PtCo@HCS-500 catalysts after pyrolysis at 500 °C. At 160 °C, a 96% yield of DMF was achieved, indicating that the catalyst is capable of catalyzing hydrogenolysis of the hydroxyl group at elevated temperatures. For hydrogenolysis of HMF to DMF, catalysts based on PtCo alloys demonstrated improved catalytic activity, and a DMF yield of 98% was achieved after 2 h of reaction.[86]

3.1.3. Valorization of Lignin Derivatives to Fuels and Biochemicals with Nanocatalysts. Lignin has low oxygen content and has become increasingly attractive for use as feedstock to produce biofuels and commodity chemicals.[87] Lignin is composed primarily of p-coumaryl, synapyl, and coniferyl alcohols linked together by C−O bonds such as α-O-4, 4-O-5, and β-O-4.[88] Many catalytic processes for selective lignin depolymerization and oxygen removal via HDO reactions have already been developed. However, some of these studies have focused on lignin model compounds rather than biomass-derived lignin. Many research groups have conducted extensive research on HDO chemistry to enhance various model compounds derived from lignin-derived bio-oils, such as vanillin, anisole, eugenol, cresol, phenol.[89−91]

Their results suggest that noble metals supported on an acidic carrier can be beneficial to catalytic systems for selective HDO processes.[89,90] Selective hydrogenolysis of aromatic C_{sp2}−O bonds is a favorable process to upgrade lignin. Nonetheless, the competing, unfavorable hydrogenation of lignin aromatic rings causes an increase H_2 consumption, resulting in less valuable saturated compounds. Before hydrogenating the aromatic rings, it is a requisite to develop catalysts that efficiently cleave the C_{sp2}−O bonds. Thus, developing catalytic strategies for the transformation of lignin to chemicals is critical for a sustainable lignocellulosic biomass biorefinery. Homogeneous Ni-based catalysts are highly selective: however, recycling them is challenging and poses problems. Various Ni-synthesized heterogeneous catalysts have been investigated for lignin hydrogenolysis recently.[100−102] Zhang et al. have demonstrated the effectiveness of bimetallic Ni catalysts with various diameters (ca. 2 nm to 4 nm) to give an excellent synergy in the hydrogenolysis of 2-phenoxy-1-phenylethanol (a lignin model compound).[103] It was also discernible that pure Ni catalysts were selective toward desired monomer products but decreased conversion, while pure Rh and Ru catalysts showed enhanced catalytic activity but decreased selectivity for target-monomer compounds.[103] Ni-bimetallic catalysts were 3- to 10-fold more active than in pure Pd, Rh, Ni, or Ru NPs in the hydrogenolysis of organosolv lignin, thereby paving the way for lignin valorization.[103,104] A recent study has reported catalytic hydrodeoxygenation of lignin bio-oil to hydrocarbons under the mild condition of temperature less than 100 °C and H_2 pressure less than 1 atm[105] (see Figure 5a,b). A triphase transfer catalytic system was employed to catalyze lignin-sourced bio-oil compounds in the HDO process.[105] SiW_{12} was used to facilitate H_2 movement from the gas phase to the aqueous reaction solution at very less H_2 pressures. The superacid SiW_{12}'s proton-associated deoxygenation mechanism significantly lowered the reaction barrier for C−O bond scission, providing the transformation of biosourced phenolic oxygenates to the desired compounds in a moderate reaction system in the presence of the Pt/C catalyst.[105] Under mild circumstances, hydrocarbon yields of up to 90% were produced by enhancing lignin bio-oil-sourced phenol derivatives and phenol. In addition, evaluation of HDO of dimer model compounds with β-O-4, α-O-4, and 4-O-5 linkages was done.[105] It was revealed that the bifunctional catalyst system was very effective at breaking the aryl ether bond[105] (see Figure 6a).

With the abundance of sunlight available on earth, the presence of photocatalysts in upgrading lignin derivatives to fuel/fuel precursors is essential to achieve a true green biorefinery setup. While TiO_2 was used for photocatalytic pollutant degradation, hydrogen evolution, and CO_2 reduction, few studies focused on photocatalytic upgrading and utilization of biomass using TiO_2. Investigation into a surface-controlled photocatalysis of TiO_2 for the selective upgrading of vanillin and furfurals was reported by Wu et al.[106] By modifying exposed facets, a different reaction pathway of the hydrogenation of the aldehyde group to C−C coupling could be achieved. In this way, aromatic alcohols and desired coupling compounds/furanics that are essential compounds or biojet fuel precursors, can be formed.[106] It has been shown that the facet-dependent density of O_2 vacancies controls the charge dispersal and adsorption strength of surface species, thereby regulating desired compound selectivity.[106] TiO_2 photocatalyst exhibited an efficient reductive transformation of vanillin and furfurals derived from lignocellulosic biomass.[106] Without surface oxygen vacancies, the catalyst preferentially catalyzes the reductive coupling process to produce C10−C18 compounds, which are

https://doi.org/10.1021/acs.iecr.1c02789
Ind. Eng. Chem. Res. 2021, 60, 18612−18626

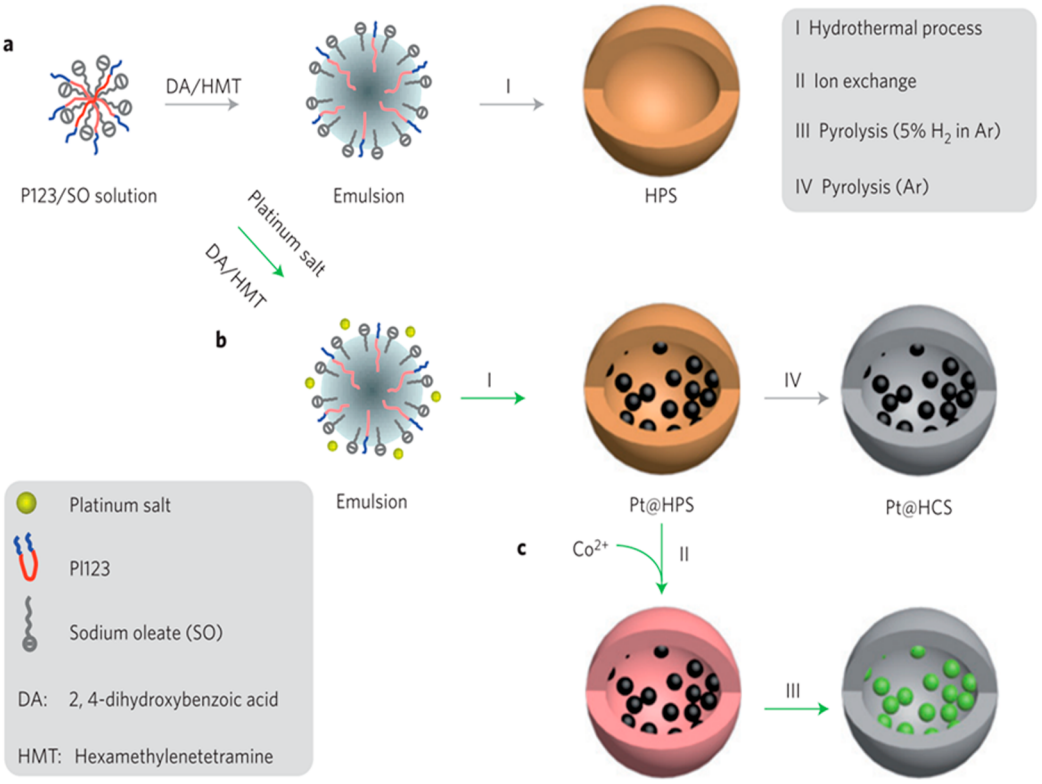

Figure 4. Synthesis of uniform hollow polymer spheres (HPS) (a); preparation of Pt@HCS (b); preparation (pyrolysis) of PtCo@HCS (c). (HCS = hhollow carbon spheres). Figure adapted with permission from ref 86. Copyright 2014 The Nature Publishing Group.

excellent biofuel precursors, while the catalyst with a high number of surface oxygen vacancies selectively catalyzes the hydrogenation of aldehyde groups to form aromatic and furanic alcohols, which are convertible commodity chemicals,[106] (see Figure 7). This result demonstrates how selectivity can be regulated by modifying TiO_2 surfaces for the purpose of valorizing biomass-derived feedstocks. The addition of value to lignin derivates as biobased polymer and polymer building blocks is a timely intervention to reduce over-reliance on petroleum sources. Even though lignin can be used directly as a building block for biopolymer production, it has some barriers due to the source of the lignin.[107] 4-Propylguaiacol is a monomer produced from lignin that is widely used. It is mostly utilized in the manufacture of polymers derived from renewable resources.[108−110]

Caprolactone and its derivatives are critical constituents of polyesters. The conversion of lignin monomers to caprolactone is a possibility[113] (see Figure 6b). Nevertheless, the most significant challenge in the conversion is the selective HDO process. Because aromatic ring hydrogenation is often carried out under severe conditions using a supported noble metal catalyst, byproduct formation is unavoidable. To address this limitation, various supported Ni catalysts using a model compound (guaiacol) were investigated.[111,112] Ni/ZrO_2 and Ni/CeO_2 showed the highest cyclohexanol yields (81%) due to their amphoteric properties, whereas neither alkaline nor acidic supports performed well.[112] Other authors observed that during a Ni/CeO_2 catalyst's high-temperature reduction (≥500 °C), partially reduced ceria moieties migrated onto Ni particles and obstructed active Ni sites.[114] By reduction of Ni on CeO_2 at a lower temperature, such Ni obstruction was avoided.[114] By decreasing the reduction temperature from 500 to 300 °C, contact times required to achieve the optimum cyclohexanol yield were substantially reduced.[112] Higher Ni loading, resulted in active catalytic sites and also increased particle size.[115,116] Increased nickel loading gave progressively larger particles, with the average particle diameter in the range of 2.5 to 20 nm as nickel loading rose from 1 wt % to 12 wt %. The TOF increased with increasing particle size, indicating a structure dependent catalyst for guaiacol transformation into cyclohexanol[112] (see Figure 6c). However, when Ni_2P (nickel phosphide) supported on either SBA-15 or SiO_2 was tested on 4-methyl guaiacol HDO, silica-supported Ni_2P catalysts had a particle size effect.[117] Large Ni_2P particles exhibited a reduced hydrogenation rate than smaller Ni_2P particles, resulting in increased cresol selectivity.[117] This is because H_2 uptake was different. Small Ni_2P clusters in combination with Bronsted acids promoted the conversion of 4-methylcyclohexanol to methylcyclohexane via a combinative dehydration−hydrogenation route.[117] The acidic/metallic nature of metal phosphide served as a bifunctional center: the metal site promoted C_{aryl-O} hydrogenolysis and hydrogenation, while the acid site promoted dehydration and transalkylation.[118−121]

Various reactions can be used to create a series of polyesters based on the ρ-hydroxycinnamic derivatives.[111,122] Depolymerization of corncob lignin using a $ZnMoO_4$/MCM-41, showed high selectivity for methyl ferulate and methyl coumarate (ca. 78%).[122] Varied catalysts ($ZnMoO_4$/MCM-41, $Zn(OAc)_2$, MCM-41, Pd/C, and Ru/C) were evaluated in a various of solvents (MeOH, EtOH, iPrOH, dioxane, THF, H_2O). Despite the excellent selectivity of ZnMoO4/MCM-41, the solvent substantially contributed to the catalyst's selectivity toward methyl coumarate and methyl ferulate esters. While MeOH, EtOH, and iPrOH favored the esters, when H_2O instead MeOH

https://doi.org/10.1021/acs.iecr.1c02789
Ind. Eng. Chem. Res. 2021, 60, 18612−18626

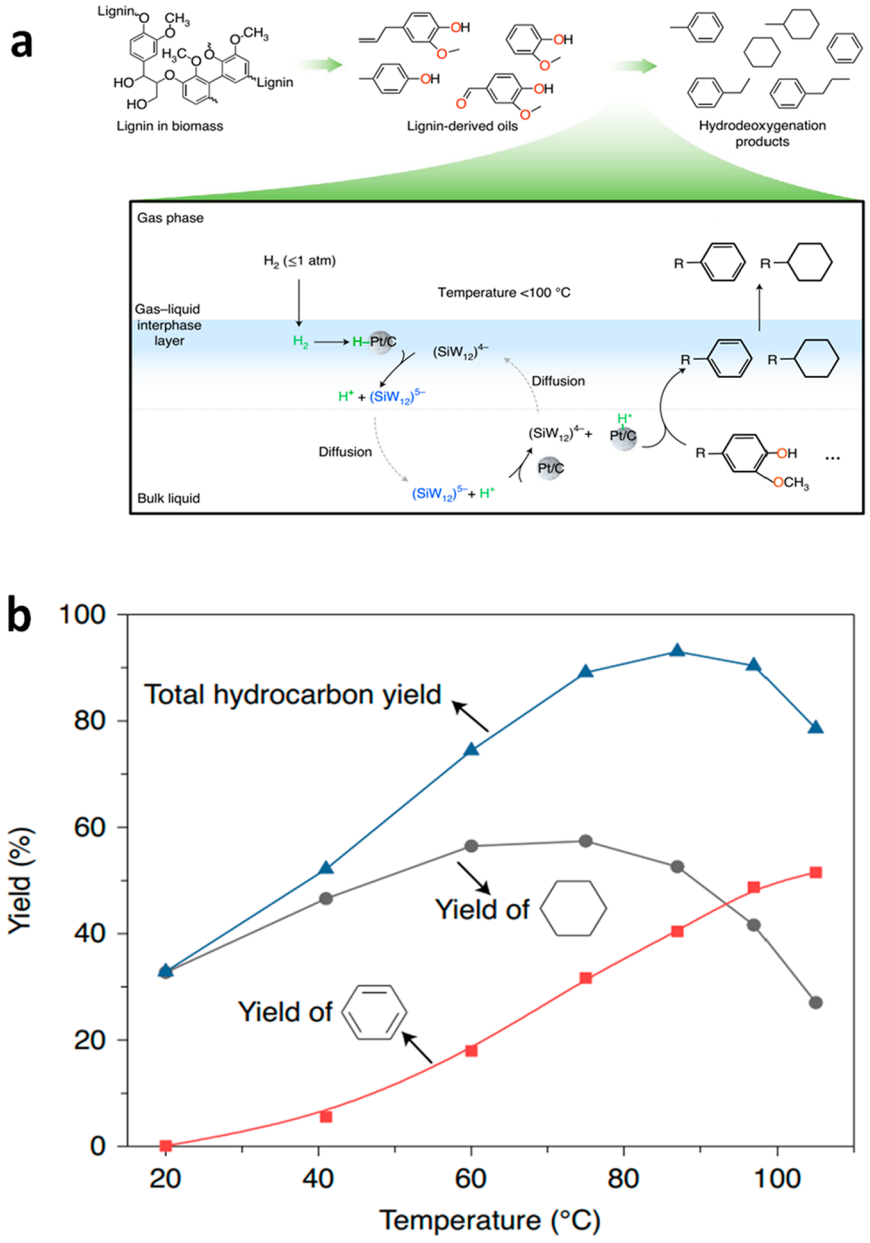

Figure 5. Representation of lignin in biomass to hydrodeoxygenation products, and proposed reaction pathway of SiW_{12} hydrogen buffer, in the presence of a Pt/C catalyst for HDO (a); HDO of phenol at different temperatures under hydrogen buffer effect and SiW_{12} and Pt/C catalyst system (b). Adapted with permission from ref105. Copyright 2021 The Nature Publishing Group.

was used as the solvent, other monomeric phenols were obtained, and no coumarate or ferulate derivatives were observed. Probably, the generated hydronium ions influenced the selectivity as argued in the literature.[122] Usually, during catalytic transformation, $ZnMoO_4$/MCM-41 exhibits high selectivity for unsaturated coumarate and ferulate derivatives.

4. NANOCATALYSTS IN BIODIESEL PRODUCTION

The most used biofuels are biodiesel, bioalcohols, biogas, bioethers, biosyngas, and high-density biofuels. There are two methods for converting biomass to biodiesel: namely, pyrolysis and transesterification. Pyrolysis is a high temperature treatment and consumes a lot of energy.[123] Transesterification is the chemical reaction between a fat/oil and alcohol (primary) that causes the formation of esters and glycerol.[124] The most common technology for producing biodiesel is transesterification of triacylglycerol and esterification of free fatty acids from plant oils or animal fats. Irrespective of the acidic or alkaline reaction mechanism, homogeneous catalysis for biodiesel generation has some limitations.[124] The process of transesterification can be performed, using acidic or alkaline catalysts. However, acid catalysts are not widely used in industry because they cause corrosion of the reactor and decrease reaction rate. Thus alkaline catalysts are more efficient than acid catalysts in the transesterification process.[125] Heterogeneous catalysts are more advantageous than homogeneous catalysts as they can be recovered following the reaction. This is because the reaction system and heterogeneous catalysts are diphasic, needing fewer washing steps to recover the catalyst.[126] However, heterogeneous catalysts pose a limitation due to deactivation of active sites through leaching.[127] Recently, a novel approach was

https://doi.org/10.1021/acs.iecr.1c02789
Ind. Eng. Chem. Res. 2021, 60, 18612−18626

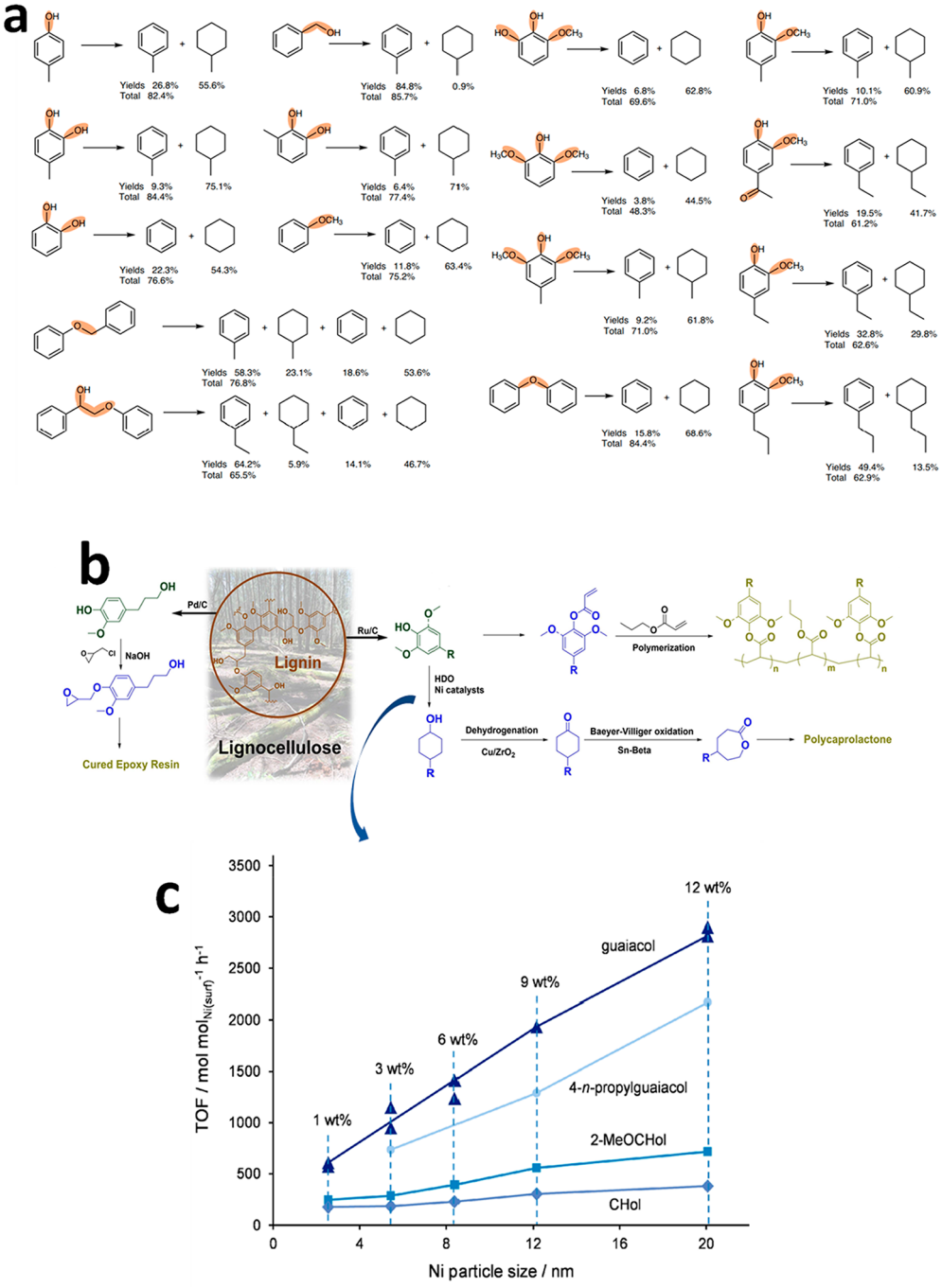

Figure 6. Enhancement of various functional-group-substituted compounds under mild conditions. Reaction condition: 0.05 mol L^{-1} SiW_{12}, Pt (5 wt %)/C, (p_{H_2} + $p_{H2O(g)}$ = 1 atm, 95 °C), Pt-to-substrate ratio = 5% (mol/mol) (a); biobased polymers from lignin monomers via lignin-first biorefinery (b); plot of the TOFs of guaiacol, 4-*n*-propylguaiacol, 2-MeOChol (2-methoxycyclohexanol), and cyclohexanol (Chol) at low conversion (<50%) against average catalyst's particle size. Ni loadings (1 to 12 wt %). TOFs of (guaiacol, 4-*n*-propylguaiacol) and (2MeOChol, cyclohexanol (Chol)) were recorded at 250 and 300 °C, respectively. Experimental conditions: decane (0.7 mmol), hexadecane (20 mL), substrate (4 mmol), 4 MPa H_2 (c). Panel a adapted with permission from ref 105. Copyright 2021 The Nature publishing Group. Panel b adapted with permission from refs 111 and 112. Copyright 2015, 2020 European Chemical Societies Publishing. Panel c adapted with permission from ref 112. Copyright 2015 European Chemical Societies Publishing.

developed, applying a coprecipitation procedure by using waste-iron-filling (WIF) as a precursor to producing α-Fe_2O_3.[128] By calcining Fe_2O_3 at temperatures of 500, 700, and 900 °C, solid acid catalysts of RBC500, RBC700, and RBC900 were formed, which were then sulfonated.[128] Average particle sizes were 259.6, 169.5, and 95.62 nm for RBC500, RBC700, and RBC900, respectively. Catalytic transesterification for 3 h at 80 °C with RBC500, RBC700, and RBC900 gave biodiesel yields of 87%, 90%, and 92%, respectively.[128] In another study, coprecipitation was used to form the CaO@ ($Sr_2Fe_2O_5$−Fe_2O_3) magnetic catalyst.[129] When compared to pure CaO, the modified CaO performed better in the production of biodiesel using soybean

https://doi.org/10.1021/acs.iecr.1c02789
Ind. Eng. Chem. Res. 2021, 60, 18612−18626

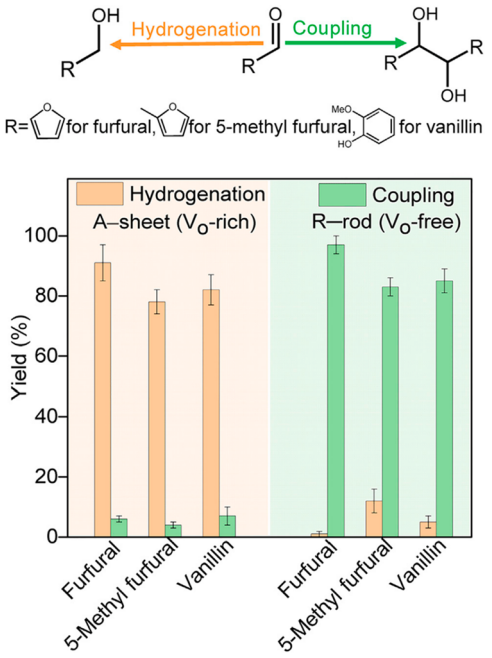

Figure 7. Catalytic upgrading of 5-methyl furfural, furfural, and vanillin by photocatalyst. Figure dapted with permission from ref 106. Copyright 2020 The Cell Press (Elsevier).

oil and methanol as raw materials. After being reused five times, the biodiesel yield could still reach 89.0% under optimal conditions indicating the stable nature of the CaO@($Sr_2Fe_2O_5$–Fe_2O_3) catalyst.[129,130] The CaO@($Sr_2Fe_2O_5$–Fe_2O_3) catalyst could be more useful in large scale application. AuNPs supported on egg shell, mussel, dolomite, calcite, and CaO were synthesized and evaluated for biodiesel production.[131] When the catalyst dose was investigated, 3% of catalyst loaded at 65 °C with a methanol/oil molar ratio of 9:1 with a reaction duration time of 3 h gave the highest oil conversion. The calcined AuNPs/CaO-based catalysts exhibited a better catalytic transesterification of sunflower oil.[131]

5. FUTURE PROSPECTS AND PERSPECTIVES

Even though HDO by heterogeneous catalysts offers tremendous potential for enhancing biomass derived fuels, it is critical to continue developing practical applications for HDO. Despite the commendable achievements in HDO of biomass-derived oxygenates, many disadvantages remain; such as the requirement for harsh reaction conditions, the application of molecular H_2 as hydrogen donor, high cost of developing the catalyst, and the low selectivity toward desired compounds. Customizing the diameter and morphology of metallic materials at the nanoregime can cause substantial changes in their structural and electronic properties, which can be much more different from those of the corresponding bulk metal catalysts. However, single-atom catalysts have been considered as the possible solution to redefining catalyst construction. One of the techniques for nanoscale engineering of the active phases is to improve physical or chemical obstacles-to-deactivation mechanisms by modifying properties of the material:[132] (1) carefully formulating the active phase which optimizes the interaction strength between the active phase and the carrier;[133,134] (2) regulating the collective characteristics of supported nanoparticles;[135,136] (3) limiting mobility by altering the energy landscape of the active phase or carrier surface.[137] Nanosized metal/metal oxides catalysts are novel, intriguing metal-based nanocatalysts discussed in this review due to their catalytic performance in biomass valorization. However, the challenge of isolating and retrieving nanoregime metal catalysts from reaction mixtures may limit their use in biomass upgrading and utilization. This problem can be solved by designing a magnetic composite nanoregime catalyst. An energy crisis is not a far-fetched scenario, and renewable biofuel will play a crucial part in our energy future by reducing our reliance on fossil fuels. Vegetal biomass is readily available and a very reassuring resource that can be converted into a wide variety of useful chemicals and fuels. However, converting lignocellulosics to fuel poses substantial challenges that require effective catalytic systems to accomplish. Hydrodeoxygenation processes may play key role in making the lignocellulosic biorefinery concept a promising tool for converting lignocellulosic biomass to liquid hydrocarbon fuels.

AUTHOR INFORMATION

Corresponding Author

Francesc Medina − *Departament d'Enginyeria Química, Universitat Rovira i Virgili, 43007 Tarragona, Spain;* orcid.org/0000-0002-3111-1542; Email: francesc.medina@urv.cat

Authors

Richard Ahorsu − *Departament d'Enginyeria Química, Universitat Rovira i Virgili, 43007 Tarragona, Spain*

Magda Constanti − *Departament d'Enginyeria Química, Universitat Rovira i Virgili, 43007 Tarragona, Spain*

Complete contact information is available at: https://pubs.acs.org/10.1021/acs.iecr.1c02789

Notes

The authors declare no competing financial interest.

ACKNOWLEDGMENTS

Richard Ahorsu is grateful for the support from Marti Franques Grant No. 2017PMF-PIPF-43. This work was supported by the Spanish Ministry of Science, Innovation and Universities, project RTI2018-098310−B-I00 and Diputació de Tarragona.

REFERENCES

(1) Ahorsu, R.; Medina, F.; Constantí, M. Significance and Challenges of Biomass as a Suitable Feedstock for Bioenergy and Biochemical Production: A Review. *Energies* **2018**, *11* (12), 3366.

(2) Chheda, J. N.; Huber, G. W.; Dumesic, J. A. Liquid-Phase Catalytic Processing of Biomass-Derived Oxygenated Hydrocarbons to Fuels and Chemicals. *Angew. Chem., Int. Ed.* **2007**, *46* (38), 7164−7183.

(3) Huber, G. W.; Iborra, S.; Corma, A. Synthesis of Transportation Fuels from Biomass Chemistry, Catalysts, and Engineering. *Chem. Rev.* **2006**, *106*, 4044−4098.

(4) Siddiki, S. M. A. H.; Touchy, A. S. Challenges and Future Prospects in Heterogeneous Catalysis for Biorefinery Technologies. In *Advanced Functional Solid Catalysts for Biomass Valorization*; Mustansar, C. H., Putla, S., Eds.; Elsevier Inc., 2020; pp 225−250.

(5) Glotov, A.; Karakhanov, E. Oil Refining. *Oil and Energy Trends* **2020**, *45* (1), 33−34.

(6) Verdoliva, V.; Saviano, M.; De Luca, S. Zeolites as Acid/Basic Solid Catalysts: Recent Synthetic Developments. *Catalysts* **2019**, *9* (3), 1−21.

(7) Rinaldi, R.; Schüth, F. Design of Solid Catalysts for the Conversion of Biomass. *Energy Environ. Sci.* **2009**, *2* (6), 610−626.

(8) Vispute, T. P.; Huber, G. W. Breaking the Chemical and Engineering Barriers to Lignocellulosic Biofuels. *Int. Sugar J.* **2008**, *110* (1311), 138−140.
(9) Schlögl, R. Heterogeneous Catalysis. *Angew. Chem., Int. Ed.* **2015**, *54* (11), 3465−3520.
(10) Newton, M. A. Dynamic Adsorbate/Reaction Induced Structural Change of Supported Metal Nanoparticles: Heterogeneous Catalysis and Beyond. *Chem. Soc. Rev.* **2008**, *37* (12), 2644−2657.
(11) Bell, A. T. The Impact of Nanoscience on Heterogeneous Catalysis. *Science* **2003**, *299* (5613), 1688−1691.
(12) Reuter, K. Ab Initio Thermodynamics and First-Principles Microkinetics for Surface Catalysis. *Catal. Lett.* **2016**, *146* (3), 541−563.
(13) Wisniak, J. The History of Catalysis. From the Beginning to Nobel Prizes. *Educ. Quim.* **2010**, *21* (1), 60−69.
(14) Lewerenz, H. J.; Heine, C.; Skorupska, K.; Szabo, N.; Hannappel, T.; Vo-Dinh, T.; Campbell, S. A.; Klemm, H. W.; Muñoz, A. G. Photoelectrocatalysis: Principles, Nanoemitter Applications and Routes to Bio-Inspired Systems. *Energy Environ. Sci.* **2010**, *3* (6), 748−760.
(15) Gates, B. C.; Huber, G. W.; Marshall, C. L.; Ross, P. N.; Siirola, J.; Wang, Y. Catalysts for Emerging Energy Applications. *MRS Bull.* **2008**, *33* (4), 429−435.
(16) Dumesic, J. A.; Huber, G. W.; Boudart, M. Introduction: Principles Of Heterogeneous Catalysis. In *Handbook of Heterogeneous Catalysis*; Ertl, G., Knözinger, H., Ferdi Schüth, J. W., Ed.; Wiley-VCH Verlag GmbH& Co. KGaA: Weinheim, Germany: Germany, 2008; pp 1−15.
(17) Nelson, A. E. Fundamentals of Industrial Catalytic Processes, 2nd Edition. C. H. Bartholomew and Robert J. Farrauto John Wiley and Sons, Hoboken, NJ, 966 pp., 2006. *Can. J. Chem.* **2008**, 127.
(18) Dumesic, J. A.; Huber, G. W.; Boudart, M. Introduction 1.1. *Handbook of Hereogeneous Catalysis*; Wiley, pp 1−15.
(19) Bartholomew, C. H.; Farrauto, R. J. Catalyst Materials, Properties and Preparation. In *Fundamentals of Industrial Catalytic Processes*; Wiley, 2010; pp 60−117.
(20) Deutschmann, O.; Knözinger, H.; Kochloefl, K.; Turek, T. Heterogeneous Catalysis and Solid Catalysts, 2. Development and Types of Solid Catalysts. *Ullmann's Encyclopedia of Industrial Chemistry*; Wiley, 2011. DOI: 10.1002/14356007.o05_o02.
(21) Muhler, M. J.; Thomas, M.; Thomas, W. J. Principles and Practice of Heterogeneous Catalysis, VCH, Weinheim, 1997, ISBN 3−527−29239-X, Preis: 88, − DM. *Berichte der Bunsengesellschaft für physikalische Chemie* **1997**, *101* (10), 1560.
(22) Gabor, A.; Somorjai, Y. L. *Introduction to Surface Chemistry and Catalysis*, 2nd ed.; Wiley: New York, 1994; Vol. *48*.
(23) Hagen, J. Background in Catalysis. In *Industrial Catalysis: A practical approach*; Hagen, J., Ed.; John Wiley and Sons, 2015; pp 1−16.
(24) Kozuch, S.; Martin, J. M. L. Turning over" Definitions in Catalytic Cycles. *ACS Catal.* **2012**, *2* (12), 2787−2794.
(25) Boudart, M. Catalysis by Supported Metals. *Adv. Catal.* **1969**, *20* (C), 153−166.
(26) Thomas, J. M.; Thomas, W. J. *Principles and Practice of Heterogeneous Catalysis*. Wiley-VCH: Weinheim, 1997; p 686.
(27) Satterfield, C. N. *Heterogeneous Catalysis in Industrial Practice*, 2nd ed.; McGraw Hill Book Co: New York, NY (United States), 1991.
(28) Bartholomew, C. H. *Fundamentals of Industrial Toxicology*; New York, 1982; Vol. *20*.
(29) Yang, Z.; Zhu, H.; Zhu, H.; Wang, Y.; Che, L.; Yang, Z.; Fang, J.; Wu, Q. H.; Chen, B. H. Insights into the Role of Nanoalloy Surface Compositions toward Catalytic Acetone Hydrogenation. *Chem. Commun.* **2018**, *54* (60), 8351−8354.
(30) Pan, J.. Facets Engineering on Catalysts. In *Heterogeneous Catalysts*; Wiley, 2021; pp 21−37.
(31) Djega-Mariadassou, G.; Boudart, M. *Kinetics of Heterogeneous Catalytic Reactions*; Princeton University Press: Princeton, NJ, 1984.
(32) Schmal, M. *Heterogeneous Catalysis and Its Industrial Applications*; Springer, 2016.
(33) Hammond, C. Intensification Studies of Heterogeneous Catalysts: Probing and Overcoming Catalyst Deactivation during Liquid Phase Operation. *Green Chem.* **2017**, *19* (12), 2711−2728.
(34) Demirbas, M. F.; Balat, M. Recent Advances on the Production and Utilization Trends of Bio-Fuels: A Global Perspective. *Energy Convers. Manage.* **2006**, *47* (15−16), 2371−2381.
(35) Yaman, S. Pyrolysis of Biomass to Produce Fuels and Chemical Feedstocks. *Energy Convers. Manage.* **2004**, *45* (5), 651−671.
(36) Li, J.; Li, N.; Qiao, Y.; Zong, P.; Wang, C.; Tian, Y.; Qin, S. Biomass Pyrolysis Liquefaction Technique: State of Research and Development Trends. *IOP Conf. Ser: Earth Environ. Sci.* **2020**, *558*, 022016.
(37) Stöcker, M. Biofuels and Biomass-to-Liquid Fuels in the Biorefinery: Catalytic Conversion of Lignocellulosic Biomass Using Porous Materials. *Angew. Chem., Int. Ed.* **2008**, *47* (48), 9200−9211.
(38) Huber, G. W.; Chheda, J. N.; Barrett, C. J.; Dumesic, J. A. Chemistry: Production of Liquid Alkanes by Aqueous-Phase Processing of Biomass-Derived Carbohydrates. *Science* **2005**, *308* (5727), 1446−1450.
(39) An, K.; Somorjai, G. A. Size and Shape Control of Metal Nanoparticles for Reaction Selectivity in Catalysis. *ChemCatChem* **2012**, *4* (10), 1512−1524.
(40) Liu, B.; Greeley, J. Decomposition Pathways of Glycerol via C-H, O-H, and C-C Bond Scission on Pt(111): A Density Functional Theory Study. *J. Phys. Chem. C* **2011**, *115* (40), 19702−19709.
(41) Li, N.; Huber, G. W. Aqueous-Phase Hydrodeoxygenation of Sorbitol with Pt/SiO2-Al2O3: Identification of Reaction Intermediates. *J. Catal.* **2010**, *270* (1), 48−59.
(42) Wawrzetz, A.; Peng, B.; Hrabar, A.; Jentys, A.; Lemonidou, A. A.; Lercher, J. A. Towards Understanding the Bifunctional Hydrodeoxygenation and Aqueous Phase Reforming of Glycerol. *J. Catal.* **2010**, *269* (2), 411−420.
(43) Zhou, C. H.; Xia, X.; Lin, C. X.; Tong, D. S.; Beltramini, J. Catalytic Conversion of Lignocellulosic Biomass to Fine Chemicals and Fuels. *Chem. Soc. Rev.* **2011**, *40* (11), 5588−5617.
(44) Kaushik, M.; Basu, K.; Benoit, C.; Cirtiu, C. M.; Vali, H.; Moores, A. Cellulose Nanocrystals as Chiral Inducers: Enantioselective Catalysis and Transmission Electron Microscopy 3D Characterization. *J. Am. Chem. Soc.* **2015**, *137* (19), 6124−6127.
(45) Zakrzewska, M. E.; Bogel-Lukasik, E.; Bogel-Lukasik, R. Ionic Liquid Mediated Formation of 5-Hydroxymethylfurfural—A Promising Biomass-Derived Building Block. *Chem. Rev.* **2011**, *111*, 397.
(46) Yu, Z.; Wu, H.; Li, Y.; Xu, Y.; Li, H.; Yang, S. Advances in Heterogeneously Catalytic Degradation of Biomass Saccharides with Ordered-Nanoporous Materials. *Ind. Eng. Chem. Res.* **2020**, *59* (39), 16970−16986.
(47) Pushkarev, V. V.; Musselwhite, N.; An, K.; Alayoglu, S.; Somorjai, G. A. High Structure Sensitivity of Vapor-Phase Furfural Decarbonylation/ Hydrogenation Reaction Network as a Function of Size and Shape of Pt Nanoparticles. *Nano Lett.* **2012**, *12* (10), 5196−5201.
(48) An, K.; Musselwhite, N.; Kennedy, G.; Pushkarev, V. V.; Robert Baker, L.; Somorjai, G. A. Preparation of Mesoporous Oxides and Their Support Effects on Pt Nanoparticle Catalysts in Catalytic Hydrogenation of Furfural. *J. Colloid Interface Sci.* **2013**, *392* (1), 122−128.
(49) Siankevich, S.; Savoglidis, G.; Fei, Z.; Laurenczy, G.; Alexander, D. T. L.; Yan, N.; Dyson, P. J. A Novel Platinum Nanocatalyst for the Oxidation of 5-Hydroxymethylfurfural into 2,5-Furandicarboxylic Acid under Mild Conditions. *J. Catal.* **2014**, *315*, 67−74.
(50) Durndell, L. J.; Zou, G.; Shangguan, W.; Lee, A. F.; Wilson, K. Structure-Reactivity Relations in Ruthenium Catalysed Furfural Hydrogenation. *ChemCatChem* **2019**, *11* (16), 3927−3932.
(51) Mondelli, C.; Gözaydin, G.; Yan, N.; Pérez-Ramírez, J. Biomass Valorisation over Metal-Based Solid Catalysts from Nanoparticles to Single Atoms. *Chem. Soc. Rev.* **2020**, *49* (12), 3764−3782.
(52) Rogers, S. M.; Catlow, C. R. A.; Chan-Thaw, C. E.; Chutia, A.; Jian, N.; Palmer, R. E.; Perdjon, M.; Thetford, A.; Dimitratos, N.; Villa, A.; et al. Tandem Site- and Size-Controlled Pd Nanoparticles for the Directed Hydrogenation of Furfural. *ACS Catal.* **2017**, *7* (4), 2266−2274.

(53) Albilali, R.; Douthwaite, M.; He, Q.; Taylor, S. H. The Selective Hydrogenation of Furfural over Supported Palladium Nanoparticle Catalysts Prepared by Sol-Immobilisation: Effect of Catalyst Support and Reaction Conditions. *Catal. Sci. Technol.* **2018**, *8* (1), 252−267.
(54) Harvey, B. G.; Merriman, W. W.; Koontz, T. A. High-Density Renewable Diesel and Jet Fuels Prepared from Multicyclic Sesquiterpanes and a 1-Hexene-Derived Synthetic Paraffinic Kerosene. *Energy Fuels* **2015**, *29* (4), 2431−2436.
(55) Xia, Q.; Chen, Z.; Shao, Y.; Gong, X.; Wang, H.; Liu, X.; Parker, S. F.; Han, X.; Yang, S.; Wang, Y. Direct Hydrodeoxygenation of Raw Woody Biomass into Liquid Alkanes. *Nat. Commun.* **2016**, *7*, 1−10.
(56) Corma, A.; Iborra, S.; Velty, A. Chemical Routes for the Transformation of Biomass into Chemicals. *Chem. Rev.* **2007**, *107*, 2411−2502.
(57) Singh, G.; Singh, L.; Gahtori, J.; Gupta, R. K.; Samanta, C.; Bal, R.; Bordoloi, A. Catalytic Hydrogenation of Furfural to Furfuryl Alcohol over Chromium-Free Catalyst: Enhanced Selectivity in the Presence of Solvent. *Mol. Catal.* **2021**, *500* (2020), 111339.
(58) Hou, P.; Ma, M.; Zhang, P.; Cao, J.; Liu, H.; Xu, X.; Yue, H.; Tian, G.; Feng, S. Catalytic Transfer Hydrogenation of Furfural to Furfuryl Alcohol Using Easy-to-Separate Core-Shell Magnetic Zirconium Hydroxide. *New J. Chem.* **2021**, *45* (5), 2715−2722.
(59) Kamble, P. A.; Kantam, M. L.; Rathod, V. K. Hydrogenation of Furfural to Furfuryl Alcohol over Nickel Supported Bentonite Catalyst. *ChemistrySelect* **2021**, *6* (25), 6601−6606.
(60) Wang, Y.; Gao, T.; Lu, Y.; Wang, Y.; Cao, Q.; Fang, W. Efficient Hydrogenation of Furfural to Furfuryl Alcohol by Magnetically Recoverable RuCo Bimetallic Catalyst. *Green Energy Environ.* **2020**, 014.
(61) Chen, J.; Sun, W.; Wang, Y.; Fang, W. Performant Au Hydrogenation Catalyst Cooperated with Cu-Doped Al2O3 for Selective Conversion of Furfural to Furfuryl Alcohol at Ambient Pressure. *Green Energy and Environment* **2021**, *6* (4), 546−556.
(62) Chen, X.; Zhang, L.; Zhang, B.; Guo, X.; Mu, X. Highly Selective Hydrogenation of Furfural to Furfuryl Alcohol over Pt Nanoparticles Supported on G-C3N4 Nanosheets Catalysts in Water. *Sci. Rep.* **2016**, *6* (April), 1−13.
(63) Villaverde, M. M.; Garetto, T. F.; Marchi, A. J. Liquid-Phase Transfer Hydrogenation of Furfural to Furfuryl Alcohol on Cu-Mg-Al Catalysts. *Catal. Commun.* **2015**, *58*, 6−10.
(64) Wu, J.; Gao, G.; Li, J.; Sun, P.; Long, X.; Li, F. Efficient and Versatile CuNi Alloy Nanocatalysts for the Highly Selective Hydrogenation of Furfural. *Appl. Catal., B* **2017**, *203*, 227−236.
(65) Guo, H.; Zhang, H.; Zhang, L.; Wang, C.; Peng, F.; Huang, Q.; Xiong, L.; Huang, C.; Ouyang, X.; Chen, X.; et al. Selective Hydrogenation of Furfural to Furfuryl Alcohol over Acid-Activated Attapulgite-Supported NiCoB Amorphous Alloy Catalyst. *Ind. Eng. Chem. Res.* **2018**, *57* (2), 498−511.
(66) Audemar, M.; Ciotonea, C.; De Oliveira Vigier, K.; Royer, S.; Ungureanu, A.; Dragoi, B.; Dumitriu, E.; Jérôme, F. Selective Hydrogenation of Furfural to Furfuryl Alcohol in the Presence of a Recyclable Cobalt/SBA-15 Catalyst. *ChemSusChem* **2015**, *8* (11), 1885−1891.
(67) Yuan, Q.; Zhang, D.; Van Haandel, L.; Ye, F.; Xue, T.; Hensen, E. J. M.; Guan, Y. Selective Liquid Phase Hydrogenation of Furfural to Furfuryl Alcohol by Ru/Zr-MOFs. *J. Mol. Catal. A: Chem.* **2015**, *406*, 58−64.
(68) Musci, J. J.; Merlo, A. B.; Casella, M. L. Aqueous Phase Hydrogenation of Furfural Using Carbon-Supported Ru and RuSn Catalysts. *Catal. Today* **2017**, *296*, 43−50.
(69) Fulajtárova, K.; Soták, T.; Hronec, M.; Vávra, I.; Dobročka, E.; Omastová, M. Aqueous Phase Hydrogenation of Furfural to Furfuryl Alcohol over Pd-Cu Catalysts. *Appl. Catal., A* **2015**, *502*, 78−85.
(70) Sun, W.; Luo, L.; Li, J.; Tian, X.; Yan, D.; Zhu, Y. Highly Efficient Hydrogenation of Furfural to Furfuryl Alcohol Catalyzed by Pt Supported on Bi-Metallic MIL-100 (Fe, Mn/Co) MOFs Derivates Prepared by Hydrothermal Polyol Reduction Method. *Catal. Lett.* **2021**, *100*, No. 0123456789.
(71) Krishnan, P. S.; Umasankar, S.; Tamizhdurai, P.; Mangesh, V. L.; Shanthi, K. Liquid Phase Hydrodeoxygenation of Furfural over Laponite Supported NiPMoS Nanocatalyst: Effect of Phosphorus Addition and Laponite Support. *J. Solid State Chem.* **2021**, *297*, 122050.
(72) Moravvej, Z.; Farshchi Tabrizi, F.; Rahimpour, M. R. Vapor Phase Conversion of Furfural to Valuable Biofuel and Chemicals Over Alumina-Supported Catalysts: Screening Catalysts. *Top. Catal.* **2021**, No. 01470-9, DOI: 10.1007/s11244-021-01470-9.
(73) Meng, X.; Wang, L.; Chen, L.; Xu, M.; Liu, N.; Zhang, J.; Yang, Y.; Wei, M. Charge-Separated Metal-Couple-Site in NiZn Alloy Catalysts towards Furfural Hydrodeoxygenation Reaction. *J. Catal.* **2020**, *392*, 69−79.
(74) Wang, Y.; Liu, F.; Han, H.; Xiao, L.; Wu, W. Metal Phosphide:A Highly Efficient Catalyst for the Selective Hydrodeoxygenation of Furfural to 2-Methylfuran. *ChemistrySelect* **2018**, *3* (27), 7926−7933.
(75) Koley, P.; Chandra Shit, S.; Joseph, B.; Pollastri, S.; Sabri, Y. M.; Mayes, E. L. H.; Nakka, L.; Tardio, J.; Mondal, J. Leveraging Cu/CuFe2O4-Catalyzed Biomass-Derived Furfural Hydrodeoxygenation: A Nanoscale Metal-Organic-Framework Template Is the Prime Key. *ACS Appl. Mater. Interfaces* **2020**, *12* (19), 21682−21700.
(76) Liu, W.; Yang, Y.; Chen, L.; Xu, E.; Xu, J.; Hong, S.; Zhang, X.; Wei, M. Atomically-Ordered Active Sites in NiMo Intermetallic Compound toward Low-Pressure Hydrodeoxygenation of Furfural. *Appl. Catal., B* **2021**, *282*, 119569.
(77) Wang, Y.; Feng, X.; Yang, S.; Xiao, L.; Wu, W. Influence of Acidity on the Catalytic Performance of Ni2P in Liquid-Phase Hydrodeoxygenation of Furfural to 2-Methylfuran. *J. Nanopart. Res.* **2020**, *22* (3), 67 DOI: 10.1007/s11051-020-04784-z.
(78) Sheng, X.; Li, G.; Wang, W.; Cong, Y.; Wang, X.; Huber, G. W.; Li, N.; Wang, A.; Zhang, T. Dual-Bed Catalyst System for the Direct Synthesis of High Density Aviation Fuel with Cyclopentanone from Lignocellulose. *AIChE J.* **2016**, *00* (00), 1−8.
(79) Li, S.; Ma, Q.; Zhong, W.; Zhao, X.; Wei, X.; Zhang, X.; Liu, Q.; Wang, C.; Ma, L.; Zhang, Q. One-Pot Hydrodeoxygenation of Bioderived Furans into Octane at Low Temperatures via an Octanediol Route. *Green Chem.* **2021**, *23*, 4741−4752.
(80) Wang, W.; Li, N.; Li, G.; Li, S.; Wang, W.; Wang, A.; Cong, Y.; Wang, X.; Zhang, T. Synthesis of Renewable High-Density Fuel with Cyclopentanone Derived from Hemicellulose. *ACS Sustainable Chem. Eng.* **2017**, *5* (2), 1812−1817.
(81) Li, D.; Ma, P.; Niu, J.; Wang, J. Recent Advances in Transition-Metal-Containing Keggin-Type Polyoxometalate-Based Coordination Polymers. *Coord. Chem. Rev.* **2019**, *392*, 49−80.
(82) De, S.; Saha, B.; Luque, R. Hydrodeoxygenation Processes: Advances on Catalytic Transformations of Biomass-Derived Platform Chemicals into Hydrocarbon Fuels. *Bioresour. Technol.* **2015**, *178*, 108−118.
(83) Li, G.; Li, N.; Wang, Z.; Li, C.; Wang, A.; Wang, X.; Cong, Y.; Zhang, T. Synthesis of High-Quality Diesel with Furfural and 2-Methylfuran from Hemicellulose. *ChemSusChem* **2012**, *5* (10), 1958−1966.
(84) Barrett, C. J.; Chheda, J. N.; Huber, G. W.; Dumesic, J. A. Single-Reactor Process for Sequential Aldol-Condensation and Hydrogenation of Biomass-Derived Compounds in Water. *Appl. Catal., B* **2006**, *66* (1−2), 111−118.
(85) Tampieri, A.; Lilic, M.; Constantí, M.; Medina, F. Microwave-Assisted Aldol Condensation of Furfural and Acetone over Mg−Al Hydrotalcite-Based Catalysts. *Crystals* **2020**, *10* (9), 1−13.
(86) Wang, G. H.; Hilgert, J.; Richter, F. H.; Wang, F.; Bongard, H. J.; Spliethoff, B.; Weidenthaler, C.; Schüth, F. Platinum-Cobalt Bimetallic Nanoparticles in Hollow Carbon Nanospheres for Hydrogenolysis of 5-Hydroxymethylfurfural. *Nat. Mater.* **2014**, *13* (3), 293−300.
(87) Ma, R.; Guo, M.; Zhang, X. Selective Conversion of Biorefinery Lignin into Dicarboxylic Acids. *ChemSusChem* **2014**, *7* (2), 412−415.
(88) Gale, M.; Cai, C. M.; Gilliard-Abdul-Aziz, K. L. Heterogeneous Catalyst Design Principles for the Conversion of Lignin into High-Value Commodity Fuels and Chemicals. *ChemSusChem* **2020**, *13* (8), 1947−1966.

(89) Runnebaum, R. C.; Nimmanwudipong, T.; Block, D. E.; Gates, B. C. Catalytic Conversion of Compounds Representative of Lignin-Derived Bio-Oils: A Reaction Network for Guaiacol, Anisole, 4-Methylanisole, and Cyclohexanone Conversion Catalysed by Pt/γ-Al 2O 3. *Catal. Sci. Technol.* **2012**, *2* (1), 113−118.
(90) Saidi, M.; Samimi, F.; Karimipourfard, D.; Nimmanwudipong, T.; Gates, B. C.; Rahimpour, M. R. Upgrading of Lignin-Derived Bio-Oils by Catalytic Hydrodeoxygenation. *Energy Environ. Sci.* **2014**, *7* (1), 103−129.
(91) Crossley, S.; Faria, J.; Shen, M.; Resasco, D. E. Solid Nanoparticles That Catalyze Biofuel Upgrade Reactions at the Water/Oil Interface. *Science* **2010**, *327* (5961), 68−72.
(92) Su, M.; Li, W.; Zhang, T.; Xin, H. S.; Li, S.; Fan, W.; Ma, L. Production of Liquid Fuel Intermediates from Furfural via Aldol Condensation over Lewis Acid Zeolite Catalysts. *Catal. Sci. Technol.* **2017**, *7* (16), 3555−3561.
(93) Kong, X.; Wei, X. j.; Li, L. p.; Fang, Z.; Lei, H. Production of Liquid Fuel Intermediates from Furfural via Aldol Condensation over La2O2CO3-ZnO-Al2O3 Catalyst. *Catal. Commun.* **2021**, *149*, 106207.
(94) Faba, L.; Díaz, E.; Ordóñez, S. Improvement of the Stability of Basic Mixed Oxides Used as Catalysts for Aldol Condensation of Bio-Derived Compounds by Palladium Addition. *Biomass Bioenergy* **2013**, *56*, 592−599.
(95) Hora, L.; Kelbichová, V.; Kikhtyanin, O.; Bortnovskiy, O.; Kubička, D. Aldol Condensation of Furfural and Acetone over MgAl Layered Double Hydroxides and Mixed Oxides. *Catal. Today* **2014**, *223*, 138−147.
(96) Kocík, J.; Frolich, K.; Perková, I.; Horáček, J. Pyroaurite-Based Mg-Fe Mixed Oxides and Their Activity in Aldol Condensation of Furfural with Acetone: Effect of Oxide Composition. *J. Chem. Technol. Biotechnol.* **2019**, *94* (2), 435−445.
(97) Desai, D. S.; Yadav, G. D. Green Synthesis of Furfural Acetone by Solvent-Free Aldol Condensation of Furfural with Acetone over La2O3-MgO Mixed Oxide Catalyst. *Ind. Eng. Chem. Res.* **2019**, *58* (35), 16096−16105.
(98) Kikhtyanin, O.; Korolova, V.; Spencer, A.; Dubnová, L.; Shumeiko, B.; Kubička, D. On the Influence of Acidic Admixtures in Furfural on the Performance of MgAl Mixed Oxide Catalysts in Aldol Condensation of Furfural and Acetone. *Catal. Today* **2021**, *367*, 248−257.
(99) Kikhtyanin, O.; Kubička, D.; Čejka, J. Toward Understanding of the Role of Lewis Acidity in Aldol Condensation of Acetone and Furfural Using MOF and Zeolite Catalysts. *Catal. Today* **2015**, *243* (C), 158−162.
(100) Sturgeon, M. R.; O'Brien, M. H.; Ciesielski, P. N.; Katahira, R.; Kruger, J. S.; Chmely, S. C.; Hamlin, J.; Lawrence, K.; Hunsinger, G. B.; Foust, T. D.; et al. Lignin Depolymerisation by Nickel Supported Layered-Double Hydroxide Catalysts. *Green Chem.* **2014**, *16* (2), 824−835.
(101) Song, Q.; Wang, F.; Xu, J. Hydrogenolysis of Lignosulfonate into Phenols over Heterogeneous Nickel Catalysts. *Chem. Commun.* **2012**, *48* (56), 7019−7021.
(102) He, J.; Zhao, C.; Lercher, J. A. Ni-Catalyzed Cleavage of Aryl Ethers in the Aqueous Phase. *J. Am. Chem. Soc.* **2012**, *134* (51), 20768−20775.
(103) Zhang, J.; Teo, J.; Chen, X.; Asakura, H.; Tanaka, T.; Teramura, K.; Yan, N. A Series of NiM (M = Ru, Rh, and Pd) Bimetallic Catalysts for Effective Lignin Hydrogenolysis in Water. *ACS Catal.* **2014**, *4* (5), 1574−1583.
(104) Zhang, J.; Asakura, H.; Van Rijn, J.; Yang, J.; Duchesne, P.; Zhang, B.; Chen, X.; Zhang, P.; Saeys, M.; Yan, N. Highly Efficient, NiAu-Catalyzed Hydrogenolysis of Lignin into Phenolic Chemicals. *Green Chem.* **2014**, *16* (5), 2432−2437.
(105) Liu, W.; You, W.; Sun, W.; Yang, W.; Korde, A.; Gong, Y.; Deng, Y. Ambient-Pressure and Low-Temperature Upgrading of Lignin Bio-Oil to Hydrocarbons Using a Hydrogen Buffer Catalytic System. *Nature Energy* **2020**, *5* (10), 759−767.
(106) Wu, X.; Li, J.; Xie, S.; Duan, P.; Zhang, H.; Feng, J.; Zhang, Q.; Cheng, J.; Wang, Y. Selectivity Control in Photocatalytic Valorization of Biomass-Derived Platform Compounds by Surface Engineering of Titanium Oxide. *Chem.* **2020**, *6* (11), 3038−3053.
(107) Sun, Z.; Fridrich, B.; De Santi, A.; Elangovan, S.; Barta, K. Bright Side of Lignin Depolymerization: Toward New Platform Chemicals. *Chem. Rev.* **2018**, *118* (2), 614−678.
(108) Koelewijn, S. F.; Cooreman, C.; Renders, T.; Andecochea Saiz, C.; Van Den Bosch, S.; Schutyser, W.; De Leger, W.; Smet, M.; Van Puyvelde, P.; Witters, H.; et al. Promising Bulk Production of a Potentially Benign Bisphenol A Replacement from a Hardwood Lignin Platform. *Green Chem.* **2018**, *20* (5), 1050−1058.
(109) Koelewijn, S. F.; Van Den Bosch, S.; Renders, T.; Schutyser, W.; Lagrain, B.; Smet, M.; Thomas, J.; Dehaen, W.; Van Puyvelde, P.; Witters, H.; et al. Sustainable Bisphenols from Renewable Softwood Lignin Feedstock for Polycarbonates and Cyanate Ester Resins. *Green Chem.* **2017**, *19* (11), 2561−2570.
(110) Ferrini, P.; Koelewijn, S. F.; Van Aelst, J.; Nuttens, N.; Sels, B. F. Zeolites as Sustainable Catalysts for the Selective Synthesis of Renewable Bisphenols from Lignin-Derived Monomers. *ChemSusChem* **2017**, *10* (10), 2249−2257.
(111) Sun, Z.; Cheng, J.; Wang, D.; Yuan, T. Q.; Song, G.; Barta, K. Downstream Processing Strategies for Lignin-First Biorefinery. *ChemSusChem* **2020**, *13* (19), 5199−5212.
(112) Schutyser, W.; Van Den Bosch, S.; Dijkmans, J.; Turner, S.; Meledina, M.; Van Tendeloo, G.; Debecker, D. P.; Sels, B. F. Selective Nickel-Catalyzed Conversion of Model and Lignin-Derived Phenolic Compounds to Cyclohexanone-Based Polymer Building Blocks. *ChemSusChem* **2015**, *8* (10), 1805−1818.
(113) Schutyser, W.; Van Den Bossche, G.; Raaffels, A.; Van Den Bosch, S.; Koelewijn, S. F.; Renders, T.; Sels, B. F. Selective Conversion of Lignin-Derivable 4-Alkylguaiacols to 4-Alkylcyclohexanols over Noble and Non-Noble-Metal Catalysts. *ACS Sustainable Chem. Eng.* **2016**, *4* (10), 5336−5346.
(114) Caballero, A.; Holgado, J. P.; Gonzalez-Delacruz, V. M.; Habas, S. E.; Herranz, T.; Salmeron, M. In Situ Spectroscopic Detection of SMSI Effect in a Ni/CeO2 System: Hydrogen-Induced Burial and Dig out of Metallic Nickel. *Chem. Commun.* **2010**, *46* (7), 1097−1099.
(115) Bond, G. C. The Origins of Particle Size Effects in Heterogeneous Catalysis. *Surf. Sci.* **1985**, *156*, 966−981.
(116) Ueno, A.; Suzuki, H.; Kotera, Y. Particle-Size Distribution of Nickel Dispersed on Silica and Its Effects on Hydrogenation of Propionaldehyde. *J. Chem. Soc., Faraday Trans. 1* **1983**, *79* (1), 127−136.
(117) Hsu, P. J.; Lin, Y. C. Hydrodeoxygenation of 4-Methylguaiacol over Silica-Supported Nickel Phosphide Catalysts: The Particle Size Effect. *J. Taiwan Inst. Chem. Eng.* **2017**, *79*, 80−87.
(118) Wu, S. K.; Lai, P. C.; Lin, Y. C. Atmospheric Hydrodeoxygenation of Guaiacol over Nickel Phosphide Catalysts: Effect of Phosphorus Composition. *Catal. Lett.* **2014**, *144* (5), 878−889.
(119) Wu, S. K.; Lai, P. C.; Lin, Y. C.; Wan, H. P.; Lee, H. T.; Chang, Y. H. Atmospheric Hydrodeoxygenation of Guaiacol over Alumina-, Zirconia-, and Silica-Supported Nickel Phosphide Catalysts. *ACS Sustainable Chem. Eng.* **2013**, *1* (3), 349−358.
(120) Sullivan, M. M.; Chen, C. J.; Bhan, A. Catalytic Deoxygenation on Transition Metal Carbide Catalysts. *Catal. Sci. Technol.* **2016**, *6* (3), 602−616.
(121) Jongerius, A. L.; Gosselink, R. W.; Dijkstra, J.; Bitter, J. H.; Bruijnincx, P. C. A.; Weckhuysen, B. M. Carbon Nanofiber Supported Transition-Metal Carbide Catalysts for the Hydrodeoxygenation of Guaiacol. *ChemCatChem* **2013**, *5* (10), 2964−2972.
(122) Wang, S.; Gao, W.; Li, H.; Xiao, L. P.; Sun, R. C.; Song, G. Selective Fragmentation of Biorefinery Corncob Lignin into P-Hydroxycinnamic Esters with a Supported Zinc Molybdate Catalyst. *ChemSusChem* **2018**, *11* (13), 2114−2123.
(123) Lira, H. N. F.; Rangel, E. T.; Suarez, P. A. Z. Diesel-Like Fuels and Lubricating Grease Preparation from an Industrial Oily Waste. *Waste Biomass Valorization* **2018**, *9* (12), 2459−2470.
(124) Thangaraj, B.; Solomon, P. R.; Muniyandi, B.; Ranganathan, S.; Lin, L. Catalysis in Biodiesel Production - A Review. *Clean Energy* **2019**, *3* (1), 2−23.

https://doi.org/10.1021/acs.iecr.1c02789
Ind. Eng. Chem. Res. 2021, 60, 18612−18626

(125) Ramirez-Ortiz, J.; Martinez, M.; Flores, H. Metakaolinite as a Catalyst for Biodiesel Production from Waste Cooking Oil. *Front. Chem. Sci. Eng.* **2012**, *6* (4), 403−409.
(126) Islam, A.; Taufiq-Yap, Y. H.; Chu, C. M.; Chan, E. S.; Ravindra, P. Studies on Design of Heterogeneous Catalysts for Biodiesel Production. *Process Saf. Environ. Prot.* **2013**, *91* (1−2), 131−144.
(127) Calero, J.; Luna, D.; Sancho, E. D.; Luna, C.; Bautista, F. M.; Romero, A. A.; Posadillo, A.; Verdugo, C. Development of a New Biodiesel That Integrates Glycerol, by Using CaO as Heterogeneous Catalyst, in the Partial Methanolysis of Sunflower Oil. *Fuel* **2014**, *122*, 94−102.
(128) Ajala, E. O.; Ajala, M. A.; Ayinla, I. K.; Sonusi, A. D.; Fanodun, S. E. Nano-Synthesis of Solid Acid Catalysts from Waste-Iron-Filling for Biodiesel Production Using High Free Fatty Acid Waste Cooking Oil. *Sci. Rep.* **2020**, *10* (1), 1−21.
(129) Zhang, P.; Shi, M.; Liu, Y.; Fan, M.; Jiang, P.; Dong, Y., Sr Doping Magnetic CaO Parcel Ferrite Improving Catalytic Activity on the Synthesis of Biodiesel by Transesterification. *Fuel* **2016**, *186*, 787−791.
(130) Wang, A.; Sudarsanam, P.; Xu, Y.; Zhang, H.; Li, H.; Yang, S. Functionalized Magnetic Nanosized Materials for Efficient Biodiesel Synthesis: Via Acid-Base/Enzyme Catalysis. *Green Chem.* **2020**, *22* (10), 2977−3012.
(131) Bet-Moushoul, E.; Farhadi, K.; Mansourpanah, Y.; Nikbakht, A. M.; Molaei, R.; Forough, M. Application of CaO-Based/Au Nanoparticles as Heterogeneous Nanocatalysts in Biodiesel Production. *Fuel* **2016**, *164*, 119−127.
(132) Goodman, E. D.; Schwalbe, J. A.; Cargnello, M. Mechanistic Understanding and the Rational Design of Sinter- Resistant Heterogeneous Catalysts. *ACS Catal.* **2017**, *7* (10), 7156−7173.
(133) Amrute, A. P.; Mondelli, C.; Schmidt, T.; Hauert, R.; Pérez-Ramírez, J. Industrial RuO2-Based Deacon Catalysts: Carrier Stabilization and Active Phase Content Optimization. *ChemCatChem* **2013**, *5* (3), 748−756.
(134) Kaiser, S. K.; Fako, E.; Manzocchi, G.; Krumeich, F.; Hauert, R.; Clark, A. H.; Safonova, O. V.; López, N.; Pérez-Ramírez, J. Nanostructuring Unlocks High Performance of Platinum Single-Atom Catalysts for Stable Vinyl Chloride Production. *Nature Catalysis* **2020**, *3* (4), 376−385.
(135) Prieto, G.; Zečević, J.; Friedrich, H.; De Jong, K. P.; De Jongh, P. E. Towards Stable Catalysts by Controlling Collective Properties of Supported Metal Nanoparticles. *Nat. Mater.* **2013**, *12* (1), 34−39.
(136) Goodman, E. D.; Johnston-Peck, A. C.; Dietze, E. M.; Wrasman, C. J.; Hoffman, A. S.; Abild-Pedersen, F.; Bare, S. R.; Plessow, P. N.; Cargnello, M. Catalyst Deactivation via Decomposition into Single Atoms and the Role of Metal Loading. *Nature Catalysis* **2019**, *2* (9), 748−755.
(137) Frei, M. S.; Mondelli, C.; García-Muelas, R.; Kley, K. S.; Puértolas, B.; López, N.; Safonova, O. V.; Stewart, J. A.; Curulla Ferré, D.; Pérez-Ramírez, J. Atomic-Scale Engineering of Indium Oxide Promotion by Palladium for Methanol Production via CO2 Hydrogenation. *Nat. Commun.* **2019**, *10* (1), 1−11.

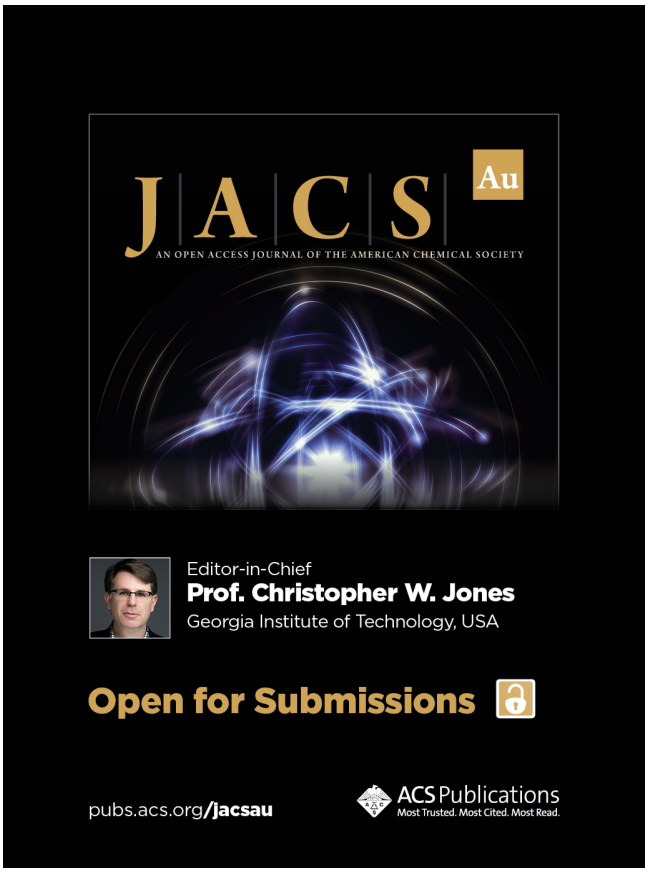

https://doi.org/10.1021/acs.iecr.1c02789
Ind. Eng. Chem. Res. 2021, 60, 18612−18626